

Forschungszentrum Karlsruhe

in der Helmholtz-Gemeinschaft

Wissenschaftliche Berichte

FZKA 6676

Validation of the Reflood Model of the RELAP5/MOD3.2.2Gamma using
Experimental Data from the Integral Facility PKL-IIB.5

Víctor Hugo Sánchez-Espinoza

Institut für Reaktorsicherheit

Programm Nukleare Sicherheitsforschung

Forschungszentrum Karlsruhe GmbH, Karlsruhe

2002

Impressum der Print-Ausgabe:

**Als Manuskript gedruckt
Für diesen Bericht behalten wir uns alle Rechte vor**

**Forschungszentrum Karlsruhe GmbH
Postfach 3640, 76021 Karlsruhe**

**Mitglied der Hermann von Helmholtz-Gemeinschaft
Deutscher Forschungszentren (HGF)**

ISSN 0947-8620

Abstract

In the framework of the Code Assessment and Maintenance Program (CAMP) of the US NRC the reflood model of the RELAP5 code is being validated at Forschungszentrum Karlsruhe (FZK) using data from the test PKL-IIB.5.

The Primärkreislauf-(PKL) test IIB.5 simulates a double-ended break of the cold leg of a German 1300 MWe PWR with emphasis on the reflood heat transfer phenomena. The PKL-facility includes all major primary coolant circuit components and some secondary components, and a containment.

After transient initiation the coolant is dumped to the containment while the ECC-systems (accumulators and low pressure injection systems) inject a large amount of cold water leading to a progressive core rewetting. Under such conditions complex heat transfer mechanisms take place in the core region.

A novel reflood model, developed at PSI, was implemented in the code version RELAP5/MOD3.2.2Gamma (322G). The heat transfer coefficient in the film and transition boiling flow regime is dependent on the distance from the quench front. The transition boiling heat transfer is predicted by the empirical Weisman correlation.

The post-test calculation of the PKL-IIB.5 test showed that the PSI-reflood model is able to describe the reflooding process in a reasonable manner. But the empirical Weisman correlation tends to over-predict the transition boiling heat transfer. Hence the semi-mechanistic FZK-transition boiling model was implemented in RELAP5 instead of the Weisman correlation. The resulting code version was named RELAP5/MOD3.2.2G+FZK (322G+FZK).

Based on the re-calculation of the PKL-test with the modified RELAP5-version it can be concluded that the rewetting temperature predicted by the FZK-transition boiling model is much closer to the experimental data than that obtained using the Weisman approach.

Results of these investigations are presented and discussed in this report.

Qualifizierung des Flutmodells im RELAP5/MOD3.2.2Gamma unter Verwendung experimenteller Daten aus der Integralanlage PKL-IIB.5

Zusammenfassung

In Rahmen des CAMP-Programms der US NRC wird das Flutmodell des Programms RELAP5 am Forschungszentrum Karlsruhe (FZK) anhand der Daten aus dem Versuch PKL-IIB5 validiert.

Der Primärkreislauf-Versuch PKL-IIB.5 simuliert einen 2F-Bruch im kalten Strang einer Hauptkühlmittelleitung eines deutschen 1300 MW_e DWR, insbesondere die Wärmeübergangsmechanismen während der Flutphase. In der PKL-Anlage sind die wichtigen Komponenten des Primärkühlkreislaufs, einige Komponente des Sekundärkreislaufes, die Bruchstelle sowie das Containment nachgebildet.

Nach Störfallbeginn werden große Primärkühlwassermengen durch das Leck in das Containment ausgeblasen. Gleichzeitig speisen die Notkühlsysteme (Druckspeicher und Niederdruck-Einspeisesysteme) so viel kaltes Wasser in den Primärkreislauf ein, dass eine progressive Kernflutung zustande kommt. Unter solchen Bedingungen spielen sich komplexe Wärmeübergangsmechanismen im Kernbereich ab.

Ein neuartiges vom PSI-entwickeltes Modell, welches diese Wärmeübergangsprozesse beschreibt, wurde in die Version RELAP5/MOD3.2.2Gamma (322G) implementiert. In diesem Modell wurde die Berechnung des Wärmeübergangs in Abhängigkeit vom Abstand zur Quenchfront im Film- und Übergangssieden eingeführt. Der Wärmeübergangskoeffizient im Übergangssiedebereich wird dabei durch die Weisman-Korrelation bestimmt.

Die Nachrechnung des Versuchs PKL-IIB.5 hat gezeigt, dass diese Version (322G) in der Lage ist, die wesentlichen Aspekte des Flutprozesses zu beschreiben. Dennoch tendiert die Weisman Korrelation dazu, den Wärmeübergang im Übergangssiedebereich zu überschätzen. Deshalb wurde das FZK-Übergangssiedemodell anstelle der Weisman-Korrelation in RELAP5 implementiert. Die neue Version wurde als RELAP5/MOD3.2.2G+FZK bezeichnet (322G+FZK).

Bei der erneuten Nachrechnung des PKL-Tests mit 322G+FZK wurden Wiederbenetzungstemperaturen berechnet, die in den verschiedenen axialen Segmenten, die eine bessere Übereinstimmung mit den Messdaten als die mit der original 322G-Version berechneten Temperaturen aufweisen.

In diesem Bericht werden Ergebnisse dieser Untersuchungen vorgestellt und diskutiert.

TABLE OF CONTENT

Table of content.....	iii
List of tables	iv
List of figures	iv
List of Abbreviations	vi
1 Introduction.....	1
2 The PKL-II B.5 experiment.....	3
2.1 Facility description.....	3
2.2 Test conduction and boundary conditions	5
3 The PKL-Model.....	7
4 Assessment of the reflood model.....	10
4.1 Results with the original version RELAP5/MOD3.2.2Gamma	10
4.1.1 System behaviour.....	10
4.1.2 Heat transfer modes and coefficients	16
4.1.3 Core thermal behaviour	18
4.2 Results with the modified version RELAP5/MOD3.2.2Gamma+FZK	27
5 Summary and conclusions	36
6 Future work.....	37
7 Literature	38
Appendix A Weisman Transition Boiling Correlation	40
Appendix B FZK-Transition Boiling Model.....	41

LIST OF TABLES

Tab. 2-1 Initial conditions for test PKL IIB5	6
Tab. 3-1 PKL-core data per zone	7
Tab. 4-1 RELAP5-Versions with different reflood models	10
Tab. 4-2 Comparison of predicted and recorded main events	11

LIST OF FIGURES

Figure 2-1 General view of the Siemens/KWU PKL test facility	4
Figure 2-2 Cross section of the PKL-core with the radial distribution of the thermocouples	5
Figure 3-1 Integral nodalization of the PKL-IIB.5 test for RELAP5	8
Figure 3-2 PKL core nodalization with the axial position of the thermocouples	9
Figure 3-3 Nodalization of the PKL fuel rod simulators	9
Figure 4-1 Predicted (lines) system pressure compared to experimental data (symbols)	12
Figure 4-2 Predicted liquid void fraction at the core bottom	12
Figure 4-3 Predicted conditioning water injection into the RPV-side, upper head, and pump-side	13
Figure 4-4 ECC-system injection to cold legs of intact loops 2 and 3	13
Figure 4-5 Comparison of predicted and measured collapsed water level	14
Figure 4-6 Comparison of predicted and measured total break outflow	14
Figure 4-7 Predicted and measured steam temperature at 2.05 m core elevation	15
Figure 4-8 Predicted and measured steam temperature at 2.05 m core elevation	15
Figure 4-9 Predicted saturation (sattemp) and vapour temperature (tempg) at core inlet	16
Figure 4-10 Predicted heat transfer modes during the pre-reflood phase at 2.05 m elevation	17
Figure 4-11 Predicted heat transfer modes during reflood phase at 1.53 m elevation	17
Figure 4-12 Predicted heat transfer coefficient at the elevation of 1.53 m	18
Figure 4-13 Comparison of predicted and measured cladding temperature	20
Figure 4-14 Predicted void fraction at core inlet	20
Figure 4-15 Comparison of predicted and measured cladding temperature	21
Figure 4-16 Predicted void fraction at 0.86 m elevation	21
Figure 4-17 Comparison of predicted and measured cladding temperature	22
Figure 4-18 Predicted void fraction	22
Figure 4-19 Comparison of predicted and measured cladding temperature	23
Figure 4-20 Predicted void fraction at 2.05 m elevation	23
Figure 4-21 Comparison of predicted and measured cladding temperature	24
Figure 4-22 Predicted void fraction in two neighbour nodes	24
Figure 4-23 Comparison of predicted and measured cladding temperature	25
Figure 4-24 Predicted void fraction in two neighbour nodes	25
Figure 4-25 Predicted integral core outlet mass outflow	26
Figure 4-26 Predicted liquid void fraction in the upper plenum	26
Figure 4-27 Comparison of RELAP5-predictions with data	28
Figure 4-28 Comparison of RELAP5-predictions with data	28
Figure 4-29 Comparison of RELAP5-predictions with data	29
Figure 4-30 Comparison of RELAP5-predictions with data	29
Figure 4-31 Comparison of RELAP5-predictions with data	30
Figure 4-32 Comparison of RELAP5-predictions with data	30

Figure 4-33	Comparison of RELAP5-predictions with data	31
Figure 4-34	Comparison of predicted and measured rewetting temperature	31
Figure 4-35	Comparison of predicted and measured rewetting temperature	32
Figure 4-36	Comparison of predicted and measured rewetting temperature	32
Figure 4-37	Predicted heat transfer coefficient at 1.53 m core elevation	33
Figure 4-38	Predicted void fraction at 1.53 m core elevation	33
Figure 4-39	Predicted heat transfer mode at 1.53 m core elevation	34
Figure 4-40	Predicted heat transfer coefficient at 3.85 m core elevation	34
Figure 4-41	Predicted void fraction at 3.85 m core elevation	35
Figure 4-42	Predicted heat transfer mode at 3.85 m core elevation	35

LIST OF ABBREVIATIONS

ACC	ACC umulator
CHF	Critical Heat Flux
CAMP	Code Assessment and Maintenance Program
EOC	End of Cycle
EOB	End Of Blowdown
ECC	Emergency Core Cooling
FZK	ForschungsZentrum Karlsruhe, Technik und Umwelt
FB	Film Boiling
INEEL	Idaho National Engineering and Environmental Laboratory, USA
IRS	Institut für ReaktorSicherheit,
ISL	Information Systems Laboratory
KWU	KraftWerk Union/Siemens
KAERI	Korean Atomic Energy Research Institute
LWR	Light Water Reactor
LOFT	Loss Of Fluid Test
LOCA	Loss Of Coolant Accident
LP	Low Pressure
LB	Large Break
LPIS	Low Pressure Injection System
NEA	Nuclear Energy Agency
OECD	Organization for Economical Cooperation and Development
PCT	Peak Cladding Temperature
PSI	Paul Scherrer Institut
PKL	PrimärKreislauf
PSF	Projekt Nukleare Sicherheitsforschung
PWR	Pressurized Water Reactor
PZR	Pressurizer
RCS	Reactor Coolant System
RPV	Reactor Pressure Vessel
RELAP	Reactor Leak and Analysis Program for LWR transients and SBLOCA
RPV	Reactor Pressure Vessel
RBHT	Rod Bundle Heat Transfer
TB	Transition Boiling
USNRC	United States Nuclear Regulatory Commission

1 Introduction

Within the international Code Assessment and Maintenance Program (CAMP) Forschungszentrum Karlsruhe (FZK) is participating in the qualification of the thermal hydraulic code RELAP5. The validation work at FZK is concentrated on the evaluation of the RELAP5-reflood model [Sanch97], [Sanch01] using data obtained from different experimental programs.

The RELAP5-code is a best-estimate thermal hydraulic code system being developed by the USNRC to analyse a wide range of plant transients and LOCAs [R5M32]. Its capability is similar to other best-estimate codes e.g. TRAC [Liles84], CATHARE [Besti96a], and ATHLET [Burw89].

The PKL IIB.5 [Schm85] test was performed by the Siemens/KWU in 1985 to study the thermal hydraulic behaviour of the primary coolant system by a large break in the cold leg. It covers the End-of-Blowdown (EOB), the refill, and the reflood phase. This test was chosen to validate the RELAP5-reflood model.

In the R5M322G-version two heat transfer packages were introduced instead of the unique package of the version R5M3.1 to simulate the heat transfer in both reflood and non-reflood situations. The reflood model of earlier code versions was extensively assessed and improved during the last decade [Anal96], [Ban99], [HCNo98], and [Sanch97]. The reflood model implemented in R5M322G was developed at PSI and has some novel features compared to the older one, e.g. the dependency of the heat transfer correlations from the distance to the quench front. The transition boiling heat transfer is modelled by the empirical Weisman correlation, [Anal96].

Since this Weisman-correlation tends to over-predict the heat transfer and hence to under-predict the cladding temperature close to the quench front, it was replaced by the FZK-transition boiling correlation. In [Sanch97] and [Sanch01] has been shown that the FZK-model gives better cladding temperature predictions the Weisman-correlation. The new code version was named RELAP5/MOD3.2.2Gamma+FZK (322G+FZK).

The FZK-approach is an extension of the phenomenological Chen-formulation that uses only local state variables predicted by the code itself and does not require other history parameters e.g. quench position, CHF or minimum film boiling temperature, [Elias98]. According to this approach the total transition boiling heat flux q_i'' is calculated as an average heat flux during the short period of contact between the liquid and the superheated wall. Hence a three-step process was postulated to describe the mechanisms of heat removal by a liquid film from the wall: 1) conduction heating of the liquid film, 2) nucleation and bubble growth within the liquid layer and 3) evaporation of a residual.

In the Appendix A and B a comparison of the Weisman correlation with the FZK-transition boiling model is given.

In this report, results of the investigations carried out to validate the PSI-model implemented in RELAP5/MOD3.2.2Gamma as well as the modified R5M322G+FZK code version will be presented and discussed.

2 The PKL-II B.5 experiment

2.1 Facility description

The Siemens Primärkreislauf (PKL) test facility was built in 1976 to investigate the behaviour of German PWRs under accidental and transient conditions. This facility simulates a Siemens-type 1300 MWe PWR and consists of a complete primary circuit including reactor pressure vessel (RPV), pressurizer (PZR) and four symmetrically arranged main coolant loops (Figure 2-1). Each loop has a fully scaled steam generator (SG) with U-tube geometry. Major parts of the secondary system without turbine and condenser are also represented. The PKL facility is a scaled 1:1 in height, 1:12 in diameter, and 1:145 in volume. The primary system pressure is limited to the maximal value of 4.5 MPa.

The PKL IIB.5[Schm85] test was carried out in 1985 by Siemens/KWU to study the thermal hydraulic behaviour of the primary system by a LB-LOCA of the cold leg. The core simulator has a total thermal power of 2.5 MW. It consists of 314 electrically heated and 26 unheated rods, respectively. They are disposed within the core in three concentric, radial zones that can be heated independently from each other, see Figure 2-2. The heater coil is ingrained in a MgO-isolation whose heat conductivity and heat capacity are similar to that of the UO₂ - pellets. The cladding is made of CrNi-steel. There is no gap between cladding and MgO-isolation. The axial power distribution of the heater rods is given by seven steps adapted to the one of the fuel rods. By this way the radial and axial power distribution of the core can be simulated. In Figure 2-2 a cross-section of the core showing the position of the thermocouples is given.

The PKL IIB.5 test was instrumented with a large number of measurement devices to get a detail information of all relevant thermal hydraulic processes during the test phase, e.g. fuel rod and coolant temperatures, mass flow rates, water levels, coolant density, coolant velocity, absolute and difference pressure as well as electrical heating power of the core simulator. On the secondary side, parameters like coolant temperature, system pressure, and water levels were recorded, too. The temperature of the cladding, wall structures and fluid is measured with NiCr-Ni-jacket thermocouples of 0.5 and 1.0 mm outer diameter, respectively. The thermocouples to measure the cladding and fluid temperature were positioned at seven axial elevations along the core height. At each axial elevation 15 thermocouples for the cladding and 10 thermocouples for the fluid were distributed within the three radial core zones (Figure 2-2).

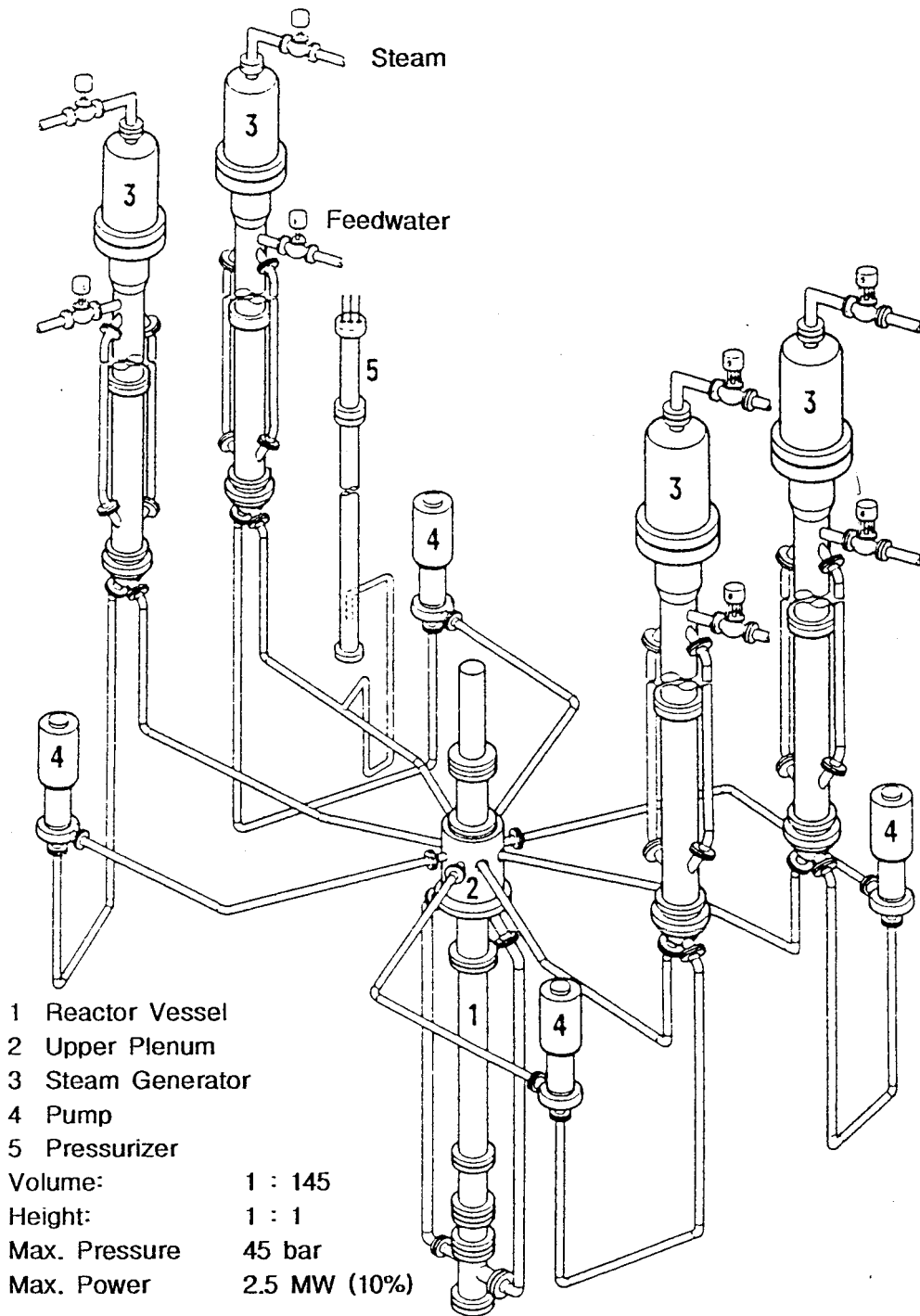


Figure 2-1 General view of the Siemens/KWU PKL test facility

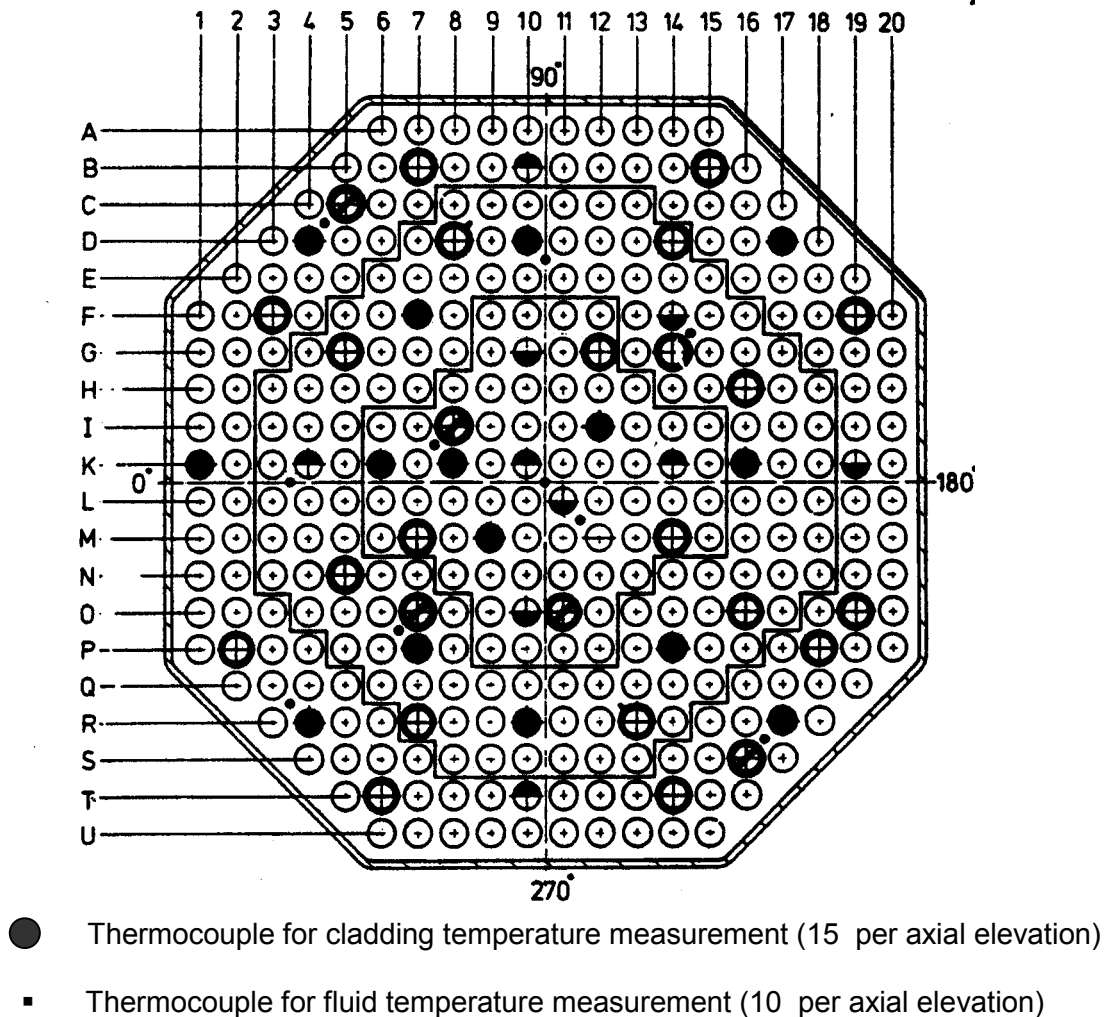


Figure 2-2 Cross section of the PKL-core with the radial distribution of the thermocouples

2.2 Test conduction and boundary conditions

In the preheating phase, the bundle is electrically heated with mean constant power supply until the predefined cladding temperature is reached. In this phase the fuel rod and steam temperature increase since no heat removal system is activated. Then the test is automatically initiated by the computer opening the break valve. At that time the primary system is filled with superheated vapour except the lower plenum of the RPV and the PZR is isolated by a valve until the break opens. Just before the break opens, conditioning water with a temperature of 523 K is injected into the upper head of the RPV and into two locations near the break (RPV-side and pump-side) to simulate the thermal hydraulic condition of the EOB-phase. This situation is so called dynamic boundary conditions, i.e. there is no initial steady state. The injection of conditioning water lasted for app.3 s.

The reflood phase starts with the activation of the accumulators (ACC) when the system pressure reduces from 4.25 MPa to values below 2.6 MPa. Further time-dependent boundary conditions like power, injection rates, etc. are controlled by the computer.

The safety injection system (ACC and LPIS) injects only into the cold legs. The LPIS begins to inject water at a temperature of 306.5 K at about 5 s after the break opens when the system pressure is below 0.5 MPa.

In Tab. 2-1 some measured PKL-parameters (initial conditions) at transient begin are listed.

Tab. 2-1 Initial conditions for test PKL IIB5

Parameter	Measurement
System pressure (MPa)	4.25
Pressurizer pressure (MPa)	7.3
Residual water in lower plenum (kg)	23
Pressurizer water mass (kg)	54
Maximal cladding temperature in inner zone (K)	927
Maximal cladding temperature central zone (K)	904
Maximal cladding temperature in outer zone (K)	895

3 The PKL-Model

A PKL-model, originally developed by Siemens/KWU for earlier RELAP5-versions, was adopted to analyse the test PKL-IIB.5 [Ban99]. The integral PKL-nodalization is based on three loops as shown in Figure 3-1. There the loop 1 and 2 are single loops (broken and intact) while loop 3 is a lumped loop including two intact single loops. The intact loops are represented in detail with hot leg, steam generator (primary/secondary side), cold leg, and pump. The PZR is linked to the intact single loop-2. The lumped intact loop-3 is also modelled in similar detail as the loop-2. The three water storage tanks are modelled as single volumes and two of them are connected to the broken loop-1 (to the pump-side and the other one to the RPV-side). The other one is connected to the RPV-dome.

The RPV model is composed of two downcomers, the lower plenum, the core and core-bypass, the upper plenum and dome (Figure 3-2). The core is represented as a single hydraulic channel with 14 axial volumes, 12 of them correspond to the active core part. The break is represented by two valves connected to an intermediate volume (number 600) which is linked to the containment. In RELAP5 the Henry-Fauske critical flow model was activated to predict the choked flow at the break using default options. In addition the abrupt area change and the non-homogeneous option were selected, too.

The fuel rod simulators are modelled as three independent heat structures representing the inner, middle and outer core zones with the parameters given in Tab. 3-1. Each fuel rod simulator is axially divided into 12 nodes and 17 radial zones as indicated in Figure 3-3. The axial positions of the thermocouples (Figure 3-2) are indicated there.

To ensure a reasonable simulation of the reflood heat transfer the axial nodes of the core simulator were allowed to be subdivided into maximal 8 fine zones (fine mesh rezoning scheme of RELAP5).

As part of the ECC-system only the LPIS-system is modelled as a time dependent volume with a time dependent junction. The ECC-system injects cold water with a temperature of 306 K to the cold legs of both intact loops 2 and 3.

Tab. 3-1 PKL-core data per zone

Items	Inner Zone	Middle Zone	Outer Zone
Number of fuel rod simulators	63	118	133
Power fraction (kW) per zone	313	502	510
Rod average power (W/rod)	4.97	4.25	3.83
Axial power shape	chopped cosine		

Preliminary RELAP5-calculations[Ban99] performed with the original PKL-model predicted a non-physical high circulation flow in the RPV-upper plenum during the preconditioning phase that may have a large impact on the PKL-initial conditions. Hence in [Ban99] the model was

modified so that the break opening time was shifted from 10.5 to 6.5 s to avoid high steam velocities.

Consequently the tables for power, safety injection, conditioning water injection, PZR-surge line opening and their trip logics were changed accordingly. With this modified input-deck reasonable steam velocities which never exceeded ± 1.5 m/s of the measured values [Ban99], were calculated.

In the PKL-calculation, the reflood model is activated when the fluid density at the core entrance is equal to or greater than the value of 735 kg/m^3 .

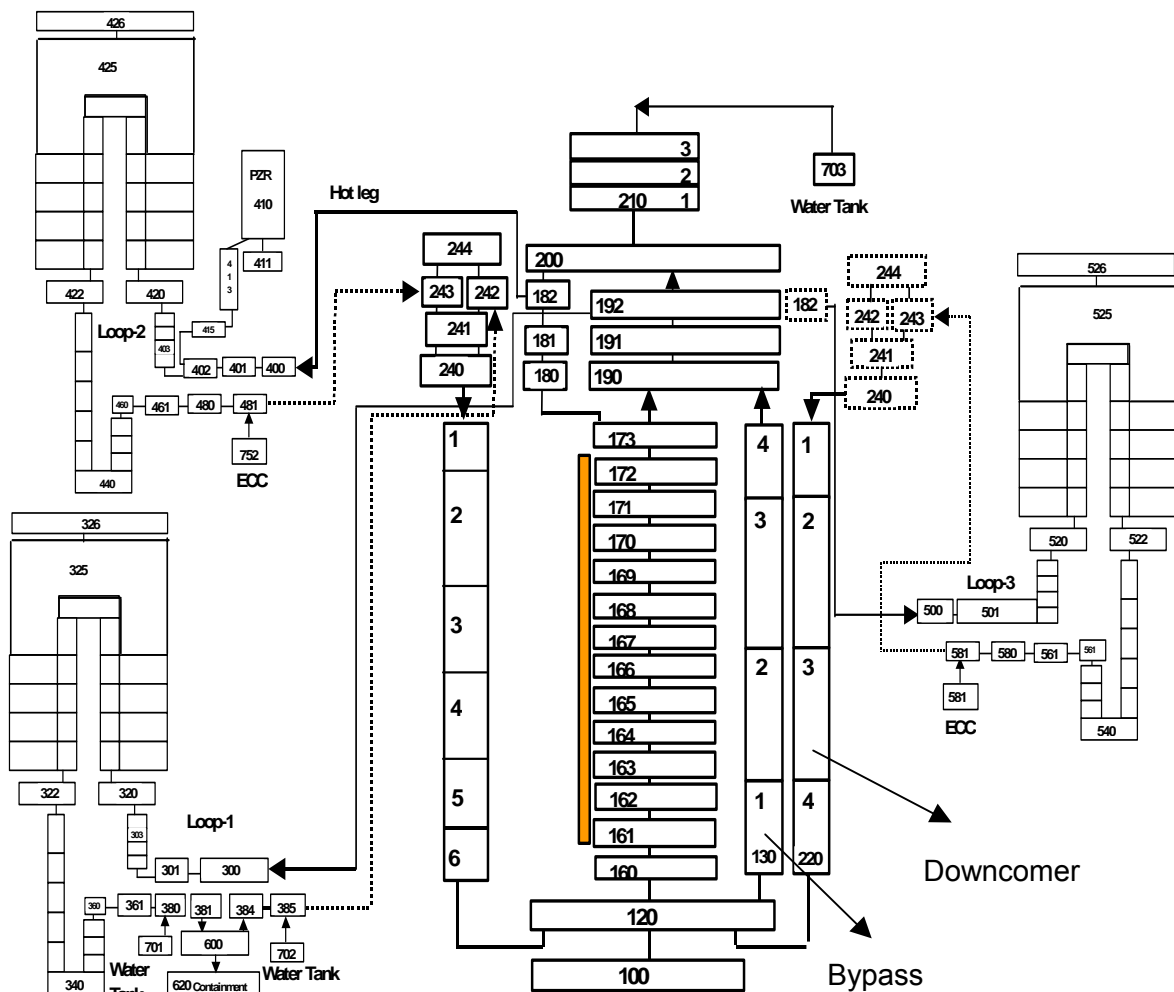


Figure 3-1 Integral nodalization of the PKL-IIB.5 test for RELAP5

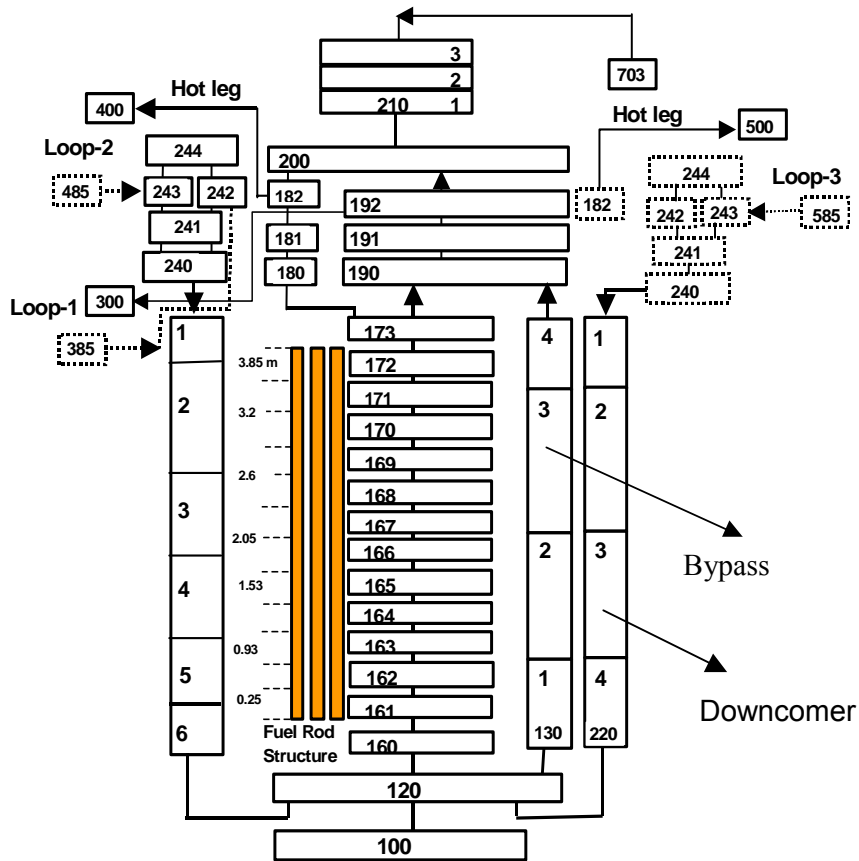


Figure 3-2 PKL core nodalization with the axial position of the thermocouples

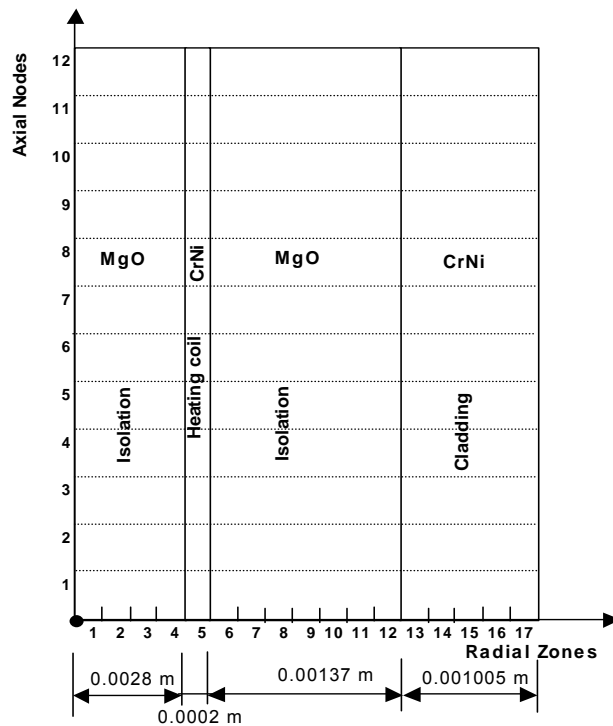


Figure 3-3 Nodalization of the PKL fuel rod simulators

4 Assessment of the reflood model

The RELAP5-reflood model is validated using the PKL IIB.5 data. The tests start with the end-of-blow-down phase and is mainly focused on the reflood phase of a LOCA. Two post-test calculations are performed with both the original 322G and the modified version 322G+FZK. In Tab. 2-1 a list of RELAP5-version with the corresponding reflood model is given.

Tab. 4-1 RELAP5-Versions with different reflood models

Code version	Reflood model	Date	Remarks
RELAP5/MOD3.1	INEEL	1994	Usable
RELAP5/MOD3.2	INEEL	1995	Not usable
RELAP5/MOD3.2.1.2	INEEL	1996	Not usable
RELAP5/MOD3.1-FZK	FZK	1997	Usable
RELAP5/MOD3.2.2 Beta	PSI	1998	Usable, but lot of errors
RELAP5/MOD3.2.2 Gamma	PSI	1999	Usable

4.1 Results with the original version RELAP5/MOD3.2.2Gamma

A post-test calculation of the PKL-test was performed with the model described in this report. Selected results of this calculation are presented and discussed here. A comparison of measured data, especially related to the core thermal behaviour, with the predictions are also given.

4.1.1 System behaviour

The sequence of main events predicted with RELAP5 is given in Tab. 4-2 and compared with the corresponding experimental values. It can be seen that data and predictions are in good agreement. The development of the system pressure in the primary and secondary coolant circuit and of the PZR predicted by the code is compared with the experimental data in Figure 4-1. They are close to each other.

The predicted liquid void fraction at the core inlet, Figure 4-2, indicates the beginning of the reflood phase. It reflects that the core bottom is filled with water after about 175 s. In Figure 4-3 the injection of the conditioning before and after transient initiation is shown. At time zero the break valve is opened. Due to sudden primary pressure reduction, the injection of ECC-systems begin early in the transient.

This is represented in Figure 4-4. Initially the injection rates to the intact single and double loops are high. Later on it is reduced to low injection rates corresponding to the LPSI-system.

As consequence of the flashing during the de-pressurization the collapsed water level experiences a rapid decrease in the initial transient phase, Figure 4-5. This trend is stopped when the outflow through the core becomes very small, Figure 4-6. Prediction and measurement shows similar trends. But there are differences during the first 25 s and at the end of the transient that is also reflected in the mass flow rate through the break (Figure 4-6) and in the fuel rod temperature.

Tab. 4-2 Comparison of predicted and recorded main events

Events	PKL-IIB.5	RELAP5/MOD3.2.2Gamma	Remarks
Break open	0 s	0 s	In calculation at 6.5 s (reset to zero)
PZR-hot line connection open	0.5 s	0.5 s	PZR emptying starts
Conditioning water Injection end	2.5 s	2.5 s	Begin at 0.5 s before break opening
ACC-injection begin	5 s	5 s	ACC stops injection at 48 s
End of blow-down	20 s	23 s	Break flow zero
Reflood model activation	--	36 s	Density at core inlet >735 kg/m ³
LPSI-injection begin	48 s	50 s	LPSI stops injection at 395 s
End of reflood phase	395 s	400 s	End of calculation

One of the reasons for the discrepancy may be the fact that the break outflow was measured far downstream from the break location while the calculated values are obtained just at the break. Hence a direct comparison of the measurement and the calculation is not so realistic.

In Figure 4-7 and Figure 4-8 a comparison of the measured and predicted steam temperatures at two axial elevations corresponding to the inner core is given. Large deviation between measured and predicted steam temperature can be observed. The experiments show a sharp steam temperature decrease to saturation conditions before quenching in some elevations. In the upper elevations no sudden steam temperature reduction (Figure 4-8) is predicted. It has to be noted that during the dispersed film boiling the calculated steam temperatures are typically below the data. This indicates that the lumped parameter model implemented in RELAP5 for dispersed film boiling has some difficulties to correctly predict the very complex heat transfer mechanisms. Since lumped parameter models treat droplets in a simple manner assuming a fixed minimum diameter, there is no chance to catch the physics. Sensitivity studies performed at FZK to investigate the influence of the droplet size on the reflood heat transfer confirmed these model limitations.

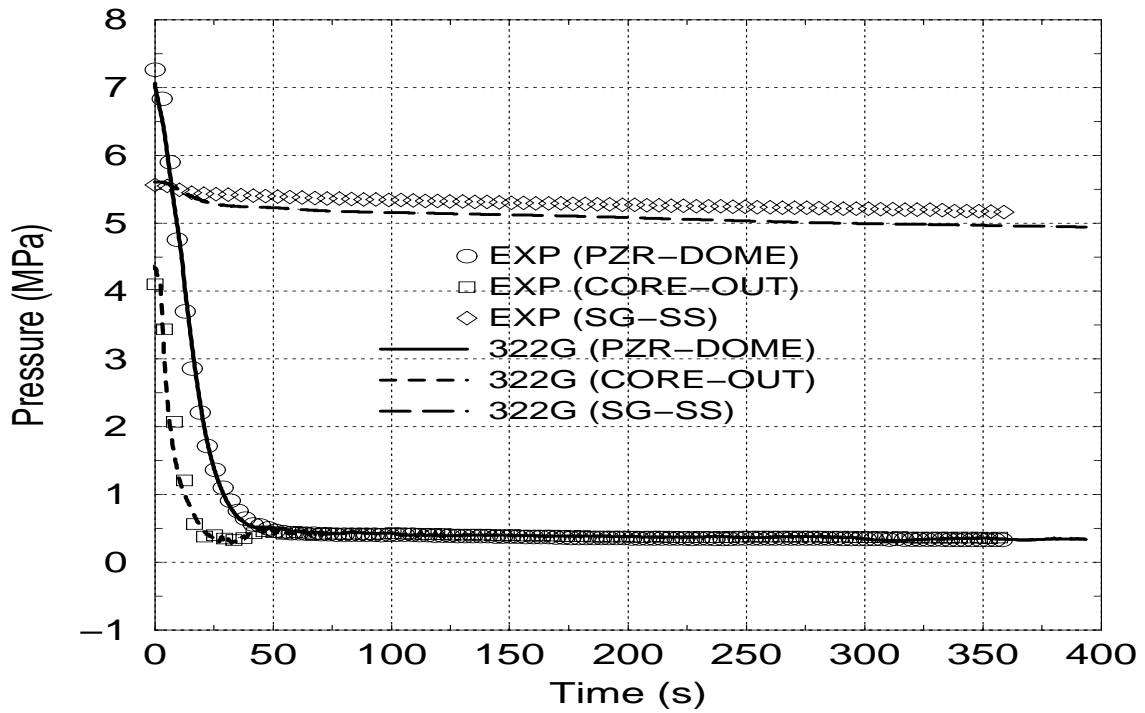


Figure 4-1 Predicted (lines) system pressure compared to experimental data (symbols)

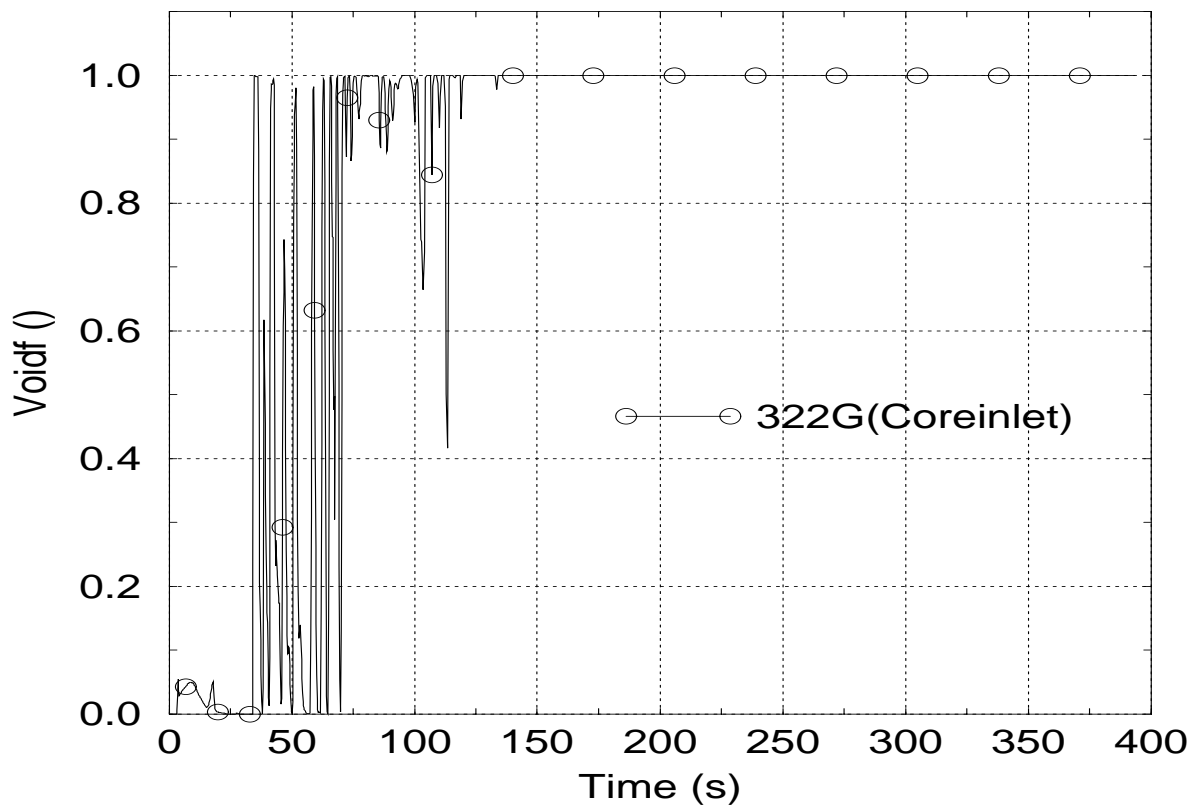


Figure 4-2 Predicted liquid void fraction at the core bottom

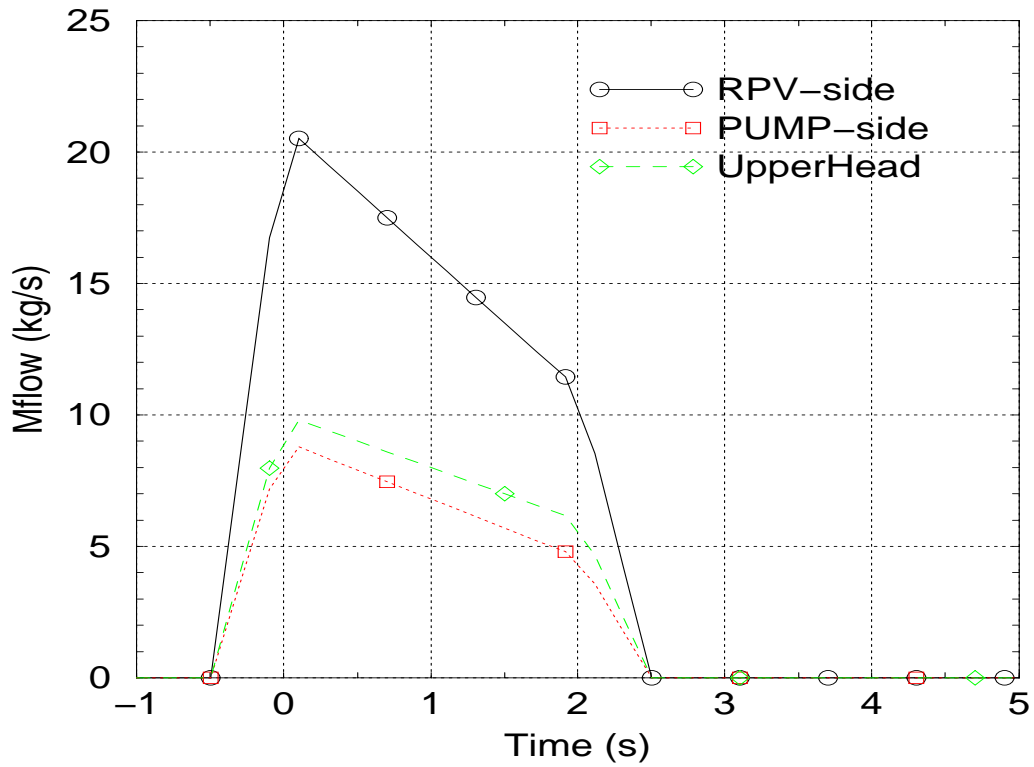


Figure 4-3 Predicted conditioning water injection into the RPV-side, upper head, and pump-side

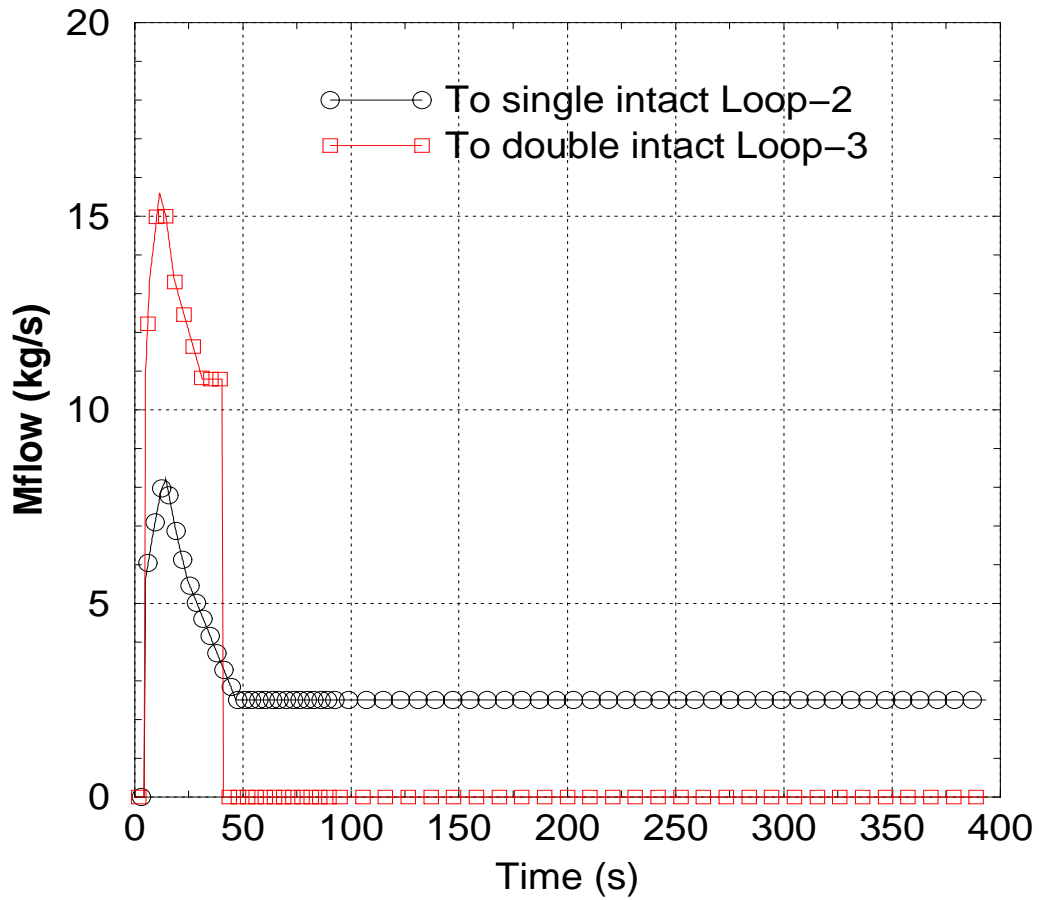


Figure 4-4 ECC-system injection to cold legs of intact loops 2 and 3

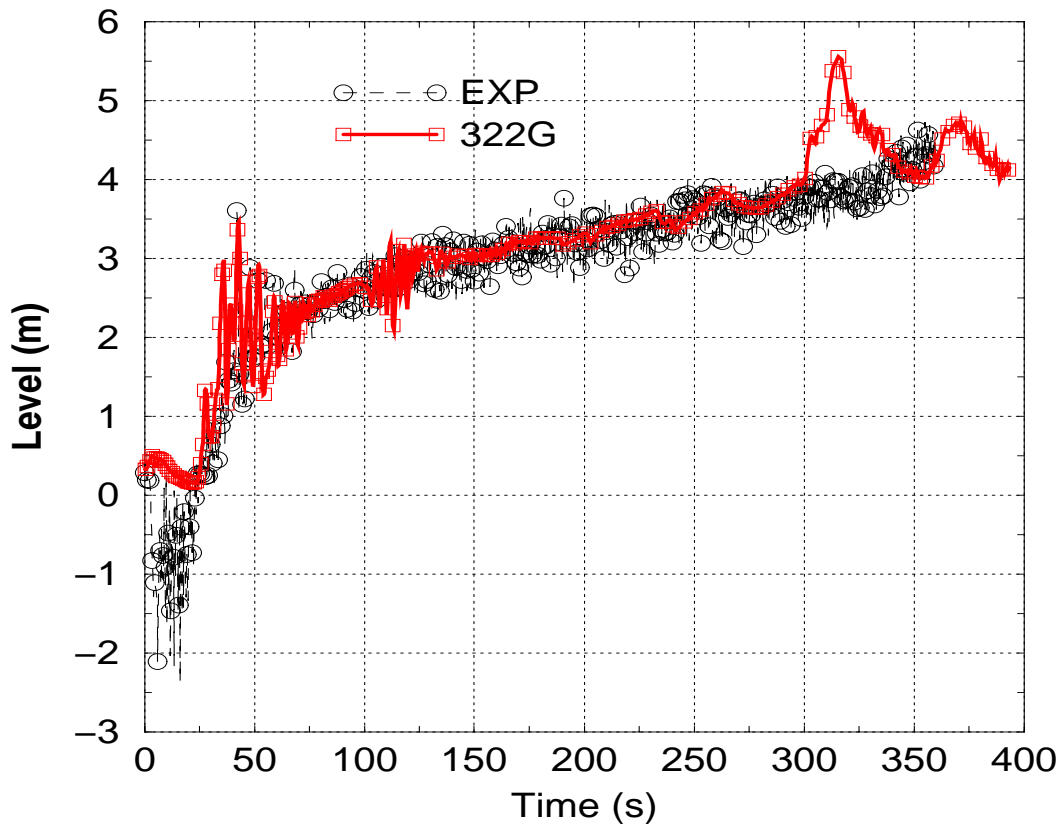


Figure 4-5 Comparison of predicted and measured collapsed water level

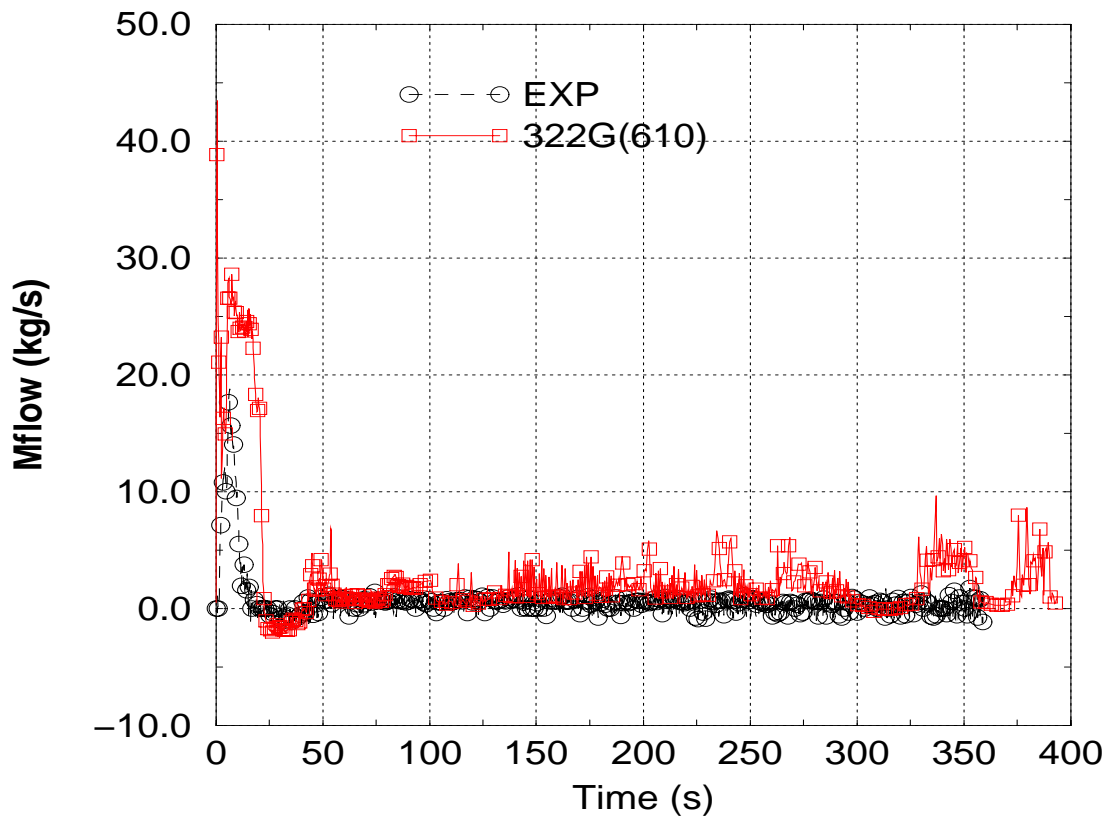


Figure 4-6 Comparison of predicted and measured total break outflow

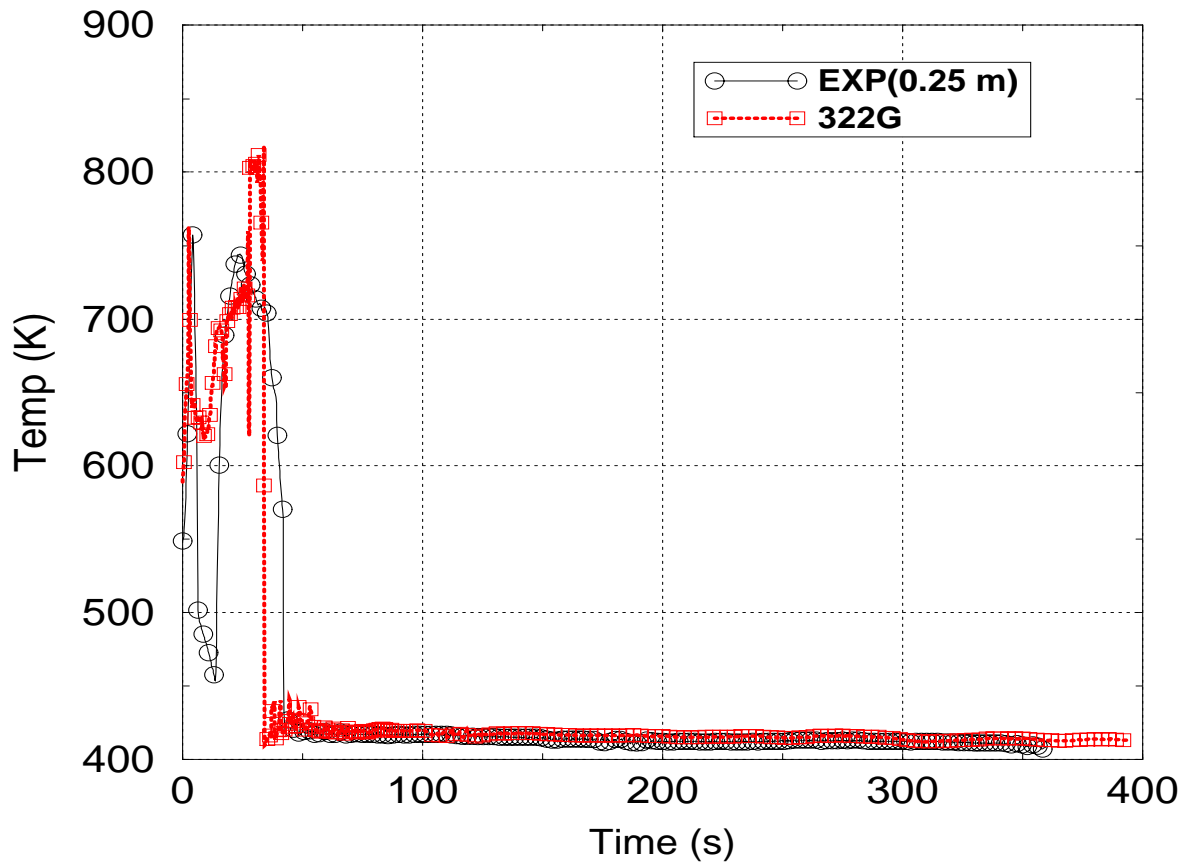


Figure 4-7 Predicted and measured steam temperature at 2.05 m core elevation

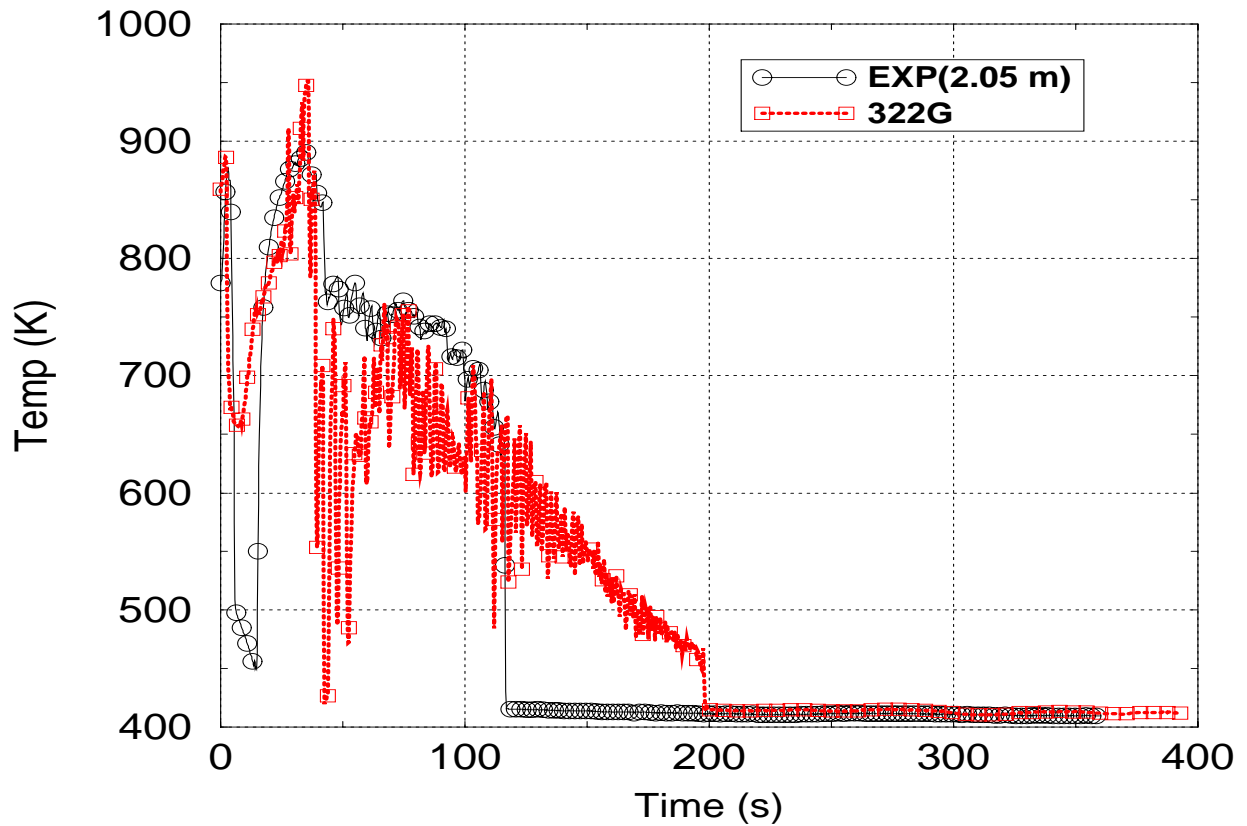


Figure 4-8 Predicted and measured steam temperature at 2.05 m core elevation

4.1.2 Heat transfer modes and coefficients

Predicted heat transfer modes and coefficients at a selected bundle height are presented and discussed hereafter. The test starts from superheated steam conditions, Figure 4-9. During this pre-reflood phase heat transfer to single phase vapour (mode 9), to film boiling (sub-cooled: mode 7, saturated mode 8), and to saturated transition boiling (mode 6) prevails, Figure 4-10. The corresponding wall-to-fluid heat transfer is determined in the non-reflood heat transfer package of RELAP5, where still the original Chen model is used even though its shortcomings were demonstrated, [Anal96] and [Sanch97]. This correlation is responsible for the cladding temperature over-prediction in the pre-reflood phase as can be seen in Figure 4-13, Figure 4-15, Figure 4-17, Figure 4-19, Figure 4-21, and Figure 4-23.

At about 35 s after transient begin the reflood model is activated in the calculation. This implies also the activation of the fine-mesh rezoning scheme and the 2D-heat conduction model for the fuel rod simulators. The heat transfer mode denotation changes by adding 40 to the original numbers. In Figure 4-11 the predicted heat transfer modes for the reflood phase is given for the bundle axial elevation of 1.53 m. It can be seen that the rod segment at this elevation undergoes dispersed film boiling (mode 48 and 47) for about 90 s before it is fully rewetted by moving quench front. The transition boiling regime (mode 46/45) is rapidly passed and finally the rod segment experiences nucleate boiling (mode 44/43) for a long time.

During the rewetting the heat transfer coefficient changes dramatically from very low values (film boiling) to high values (transition and nucleate boiling) as shown in Figure 4-12. This high heat transfer coefficient determines the rapid cladding temperature reduction with the prominent knee-temperature. Later on this so called “knee-temperature” will be clearly observed in both predictions and data.

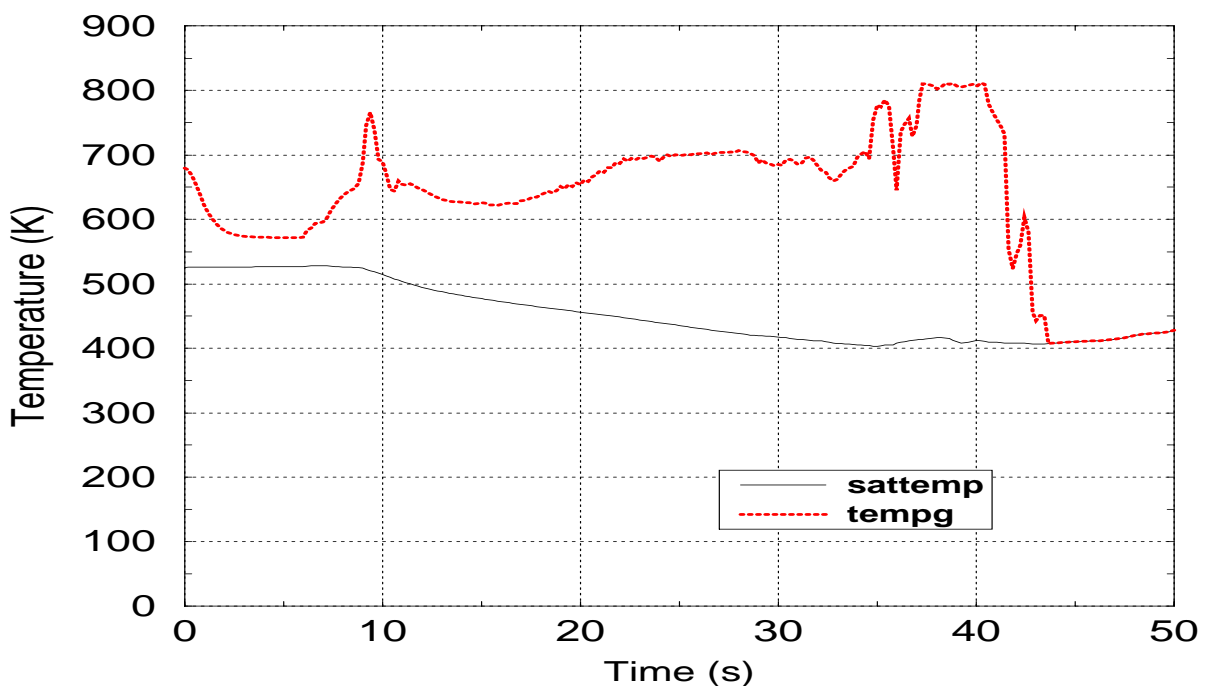


Figure 4-9 Predicted saturation (sattemp) and vapour temperature (tempg) at core inlet

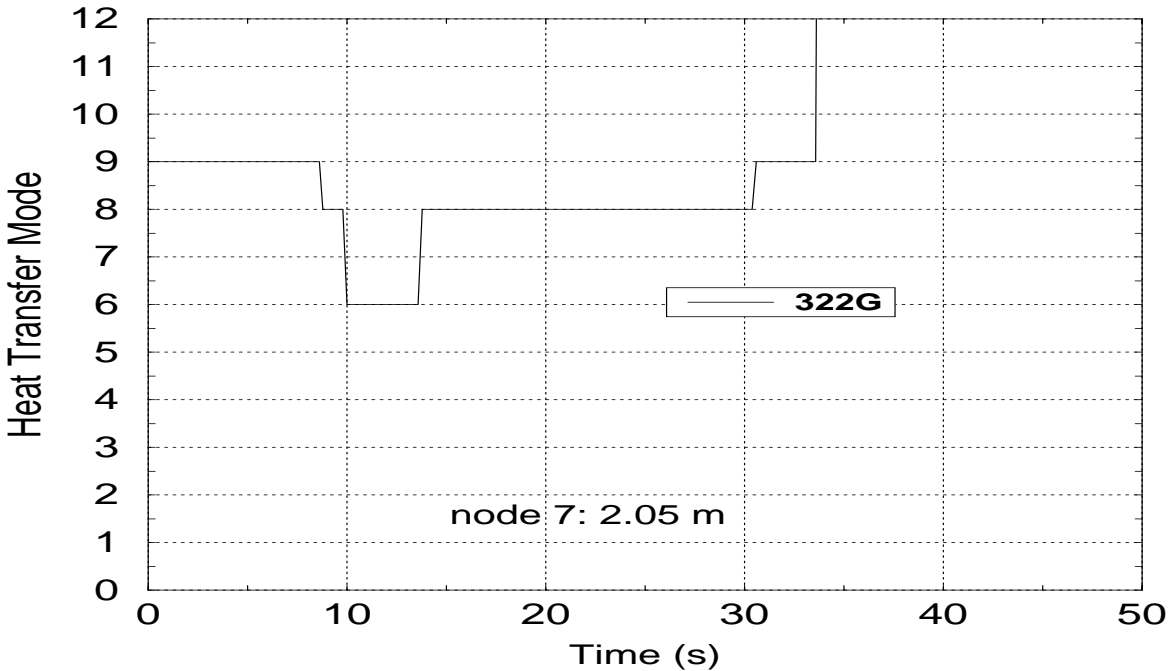


Figure 4-10 Predicted heat transfer modes during the pre-reflood phase at 2.05 m elevation

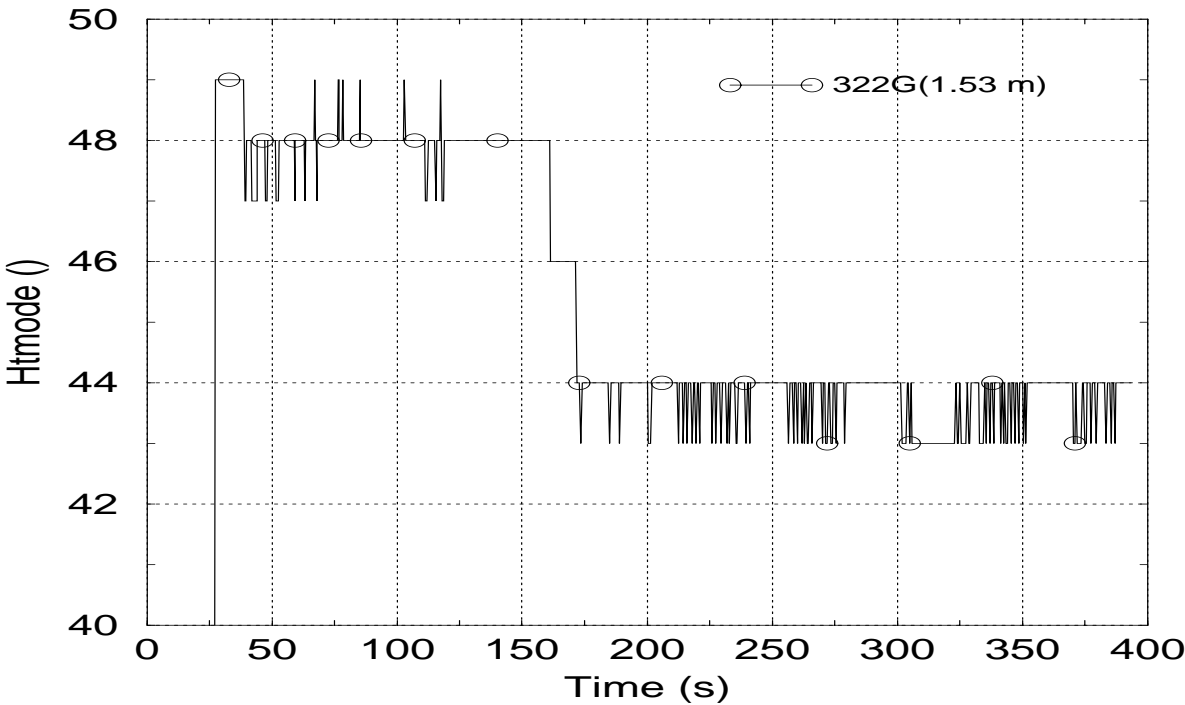


Figure 4-11 Predicted heat transfer modes during reflood phase at 1.53 m elevation

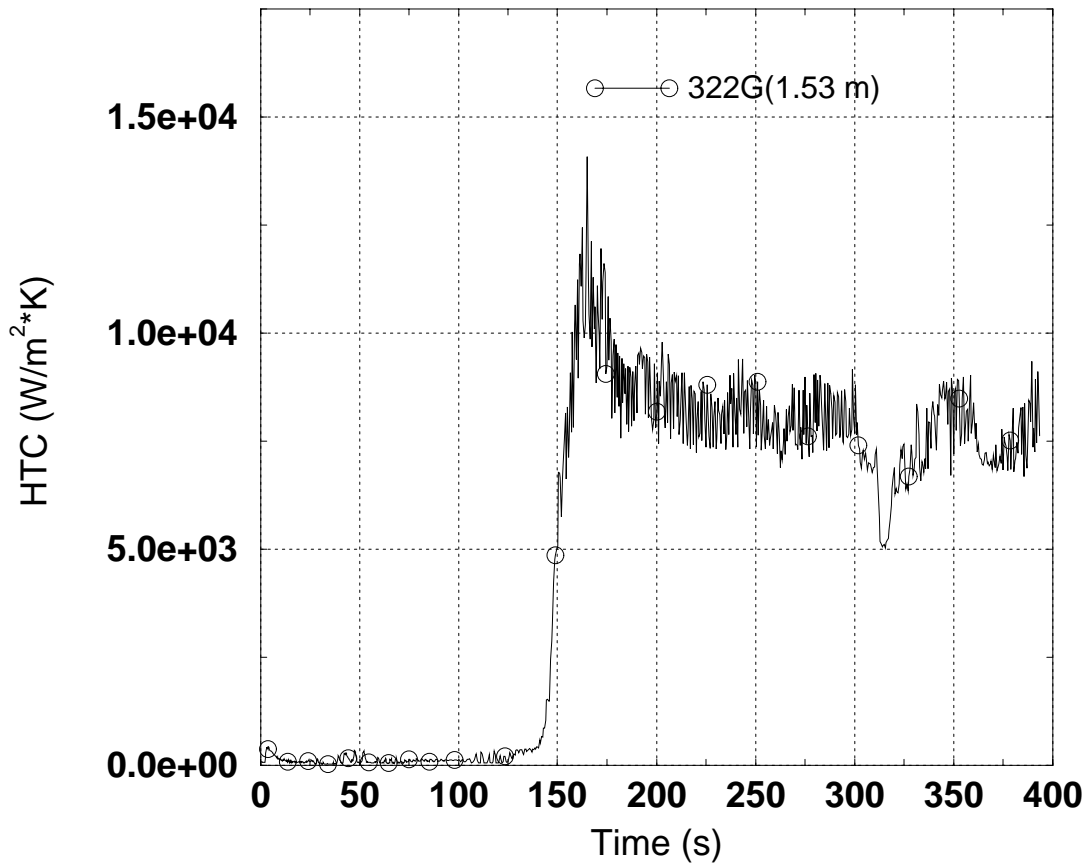


Figure 4-12 Predicted heat transfer coefficient at the elevation of 1.53 m

4.1.3 Core thermal behaviour

The core thermal response is discussed comparing the code predictions with the test data, i.e. the cladding temperature at several elevations of the central bundle. It has to be noted that several thermocouples were distributed within the core at each axial elevation. Hence the predicted cladding temperature (named 322G) is compared with all available and usable thermocouples records measured at the same elevation (named EXP), i.e. all temperature curves with the name EXP correspond to different thermocouples radially distributed at the same axial elevation.

The predicted cladding temperature is compared to the measurements in Figure 4-13, Figure 4-15, Figure 4-17, Figure 4-19, Figure 4-21, and Figure 4-23 at different axial elevations. At each axial elevation, the void fraction predicted by RELAP5 is given in Figure 4-14, Figure 4-16, Figure 4-18, Figure 4-20, Figure 4-22, and Figure 4-24.

In Figure 4-14 can be seen that the void fraction during the pre-reflood phase is close to 1 and it undergoes a strong reduction when the quench front starts to be rewetted (elevation 0.25 m). The rewetting of a bundle segment is characterized by a sudden cladding temperature reduction as can be seen in all temperature curves. This is caused by the enlarged heat transfer coefficient in the transition and nucleate boiling flow regime compared to the film boiling one.

The cladding temperature is always over-predicted during the pre-quench phase in almost all axial segments due to the original Chen-correlation which is still part of the non-reflood heat transfer package in RELAP5.

The cladding temperature curves calculated for the reflood phase have shown that RELAP5 is able to predict the overall trend of the cladding temperature in most axial elevations with a reasonable accuracy, especially during the film boiling flow regime. The agreement is very good in the middle bundle elevation, Figure 4-19. But it is not the case for the upper bundle part (Figure 4-23). The discrepancy between predictions and measurements becomes larger even though the trends are similar.

Close to the quench front RELAP5 predicts qualitatively similar trend than measured data but the temperature reduction before the sharp decrease is more pronounced in the calculations than in the measurements. Moreover the predicted rewetting temperature is much lower than the measured ones, which averages around 700 K. This under-prediction of the quench temperature by the original 322G-version is attributed to the empirical Weisman transition boiling correlation of the PSI-reflood model. For the upper bundle elevation (3.85 m) the original version 322G was not able to predict a quench-like temperature trend. It is worth to mention that the thermocouples at that elevation recorded similar trends only for the 150 s. Later on the quench time of each thermocouple is different. It must be noted that the thermocouples at the bundle elevations of 3.19 m and 3.85 m were not located at the centre of the calculation node but at the border line of neighbour nodes, so that the temperature predicted in both neighbour nodes were plotted for comparison purposes, Figure 4-21, Figure 4-23.

In Figure 4-25 the integrated coolant mass outflow at core outlet (steam and liquid) predicted by 322G is presented. It can be seen that with the begin of LPSI-injection the amount of entrained droplets increases considerable (before 50 s). Then a steady increase of both steam and liquid is predicted the transient progression. Moreover in Figure 4-26 an increased droplets entrainment is noted in the upper plenum coincident with the reflood phase initiation and later on, around 300 s, when the bundle is completed rewetted. One reason for the considerable entrainment of droplets into the upper plenum is attributed to the reduction of the droplets diameter in the model that predicts dispersed film boiling in RELAP5/MOD3.2.2Gamma compared to RELAP5/MOD3.1 from 3 mm to 1.5 mm.

From the presented results can be concluded that RELAP5/MOD3.2.2Gamma is appropriate to simulate the reflood heat transfer in an acceptable manner. The overall trend of the cladding temperature in most elevations is similar to the data. But the transition boiling heat transfer is over-predicted by the Weisman correlation leading to low rewetting temperatures.

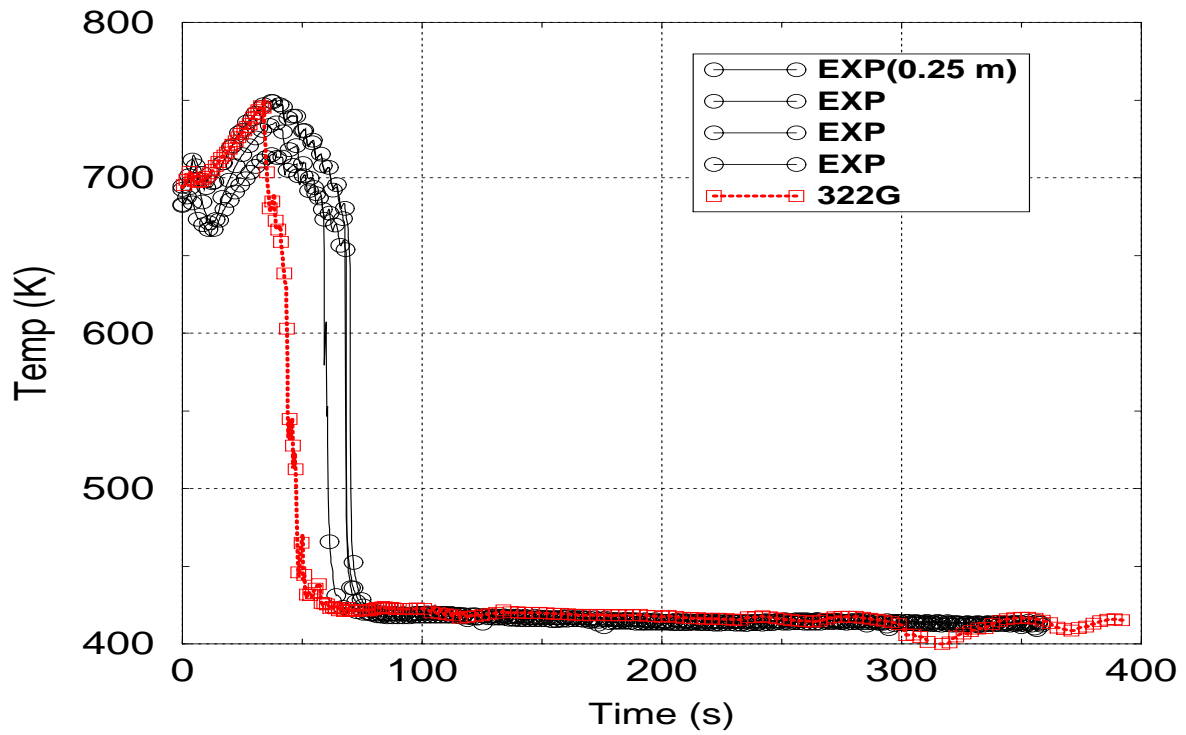


Figure 4-13 Comparison of predicted and measured cladding temperature

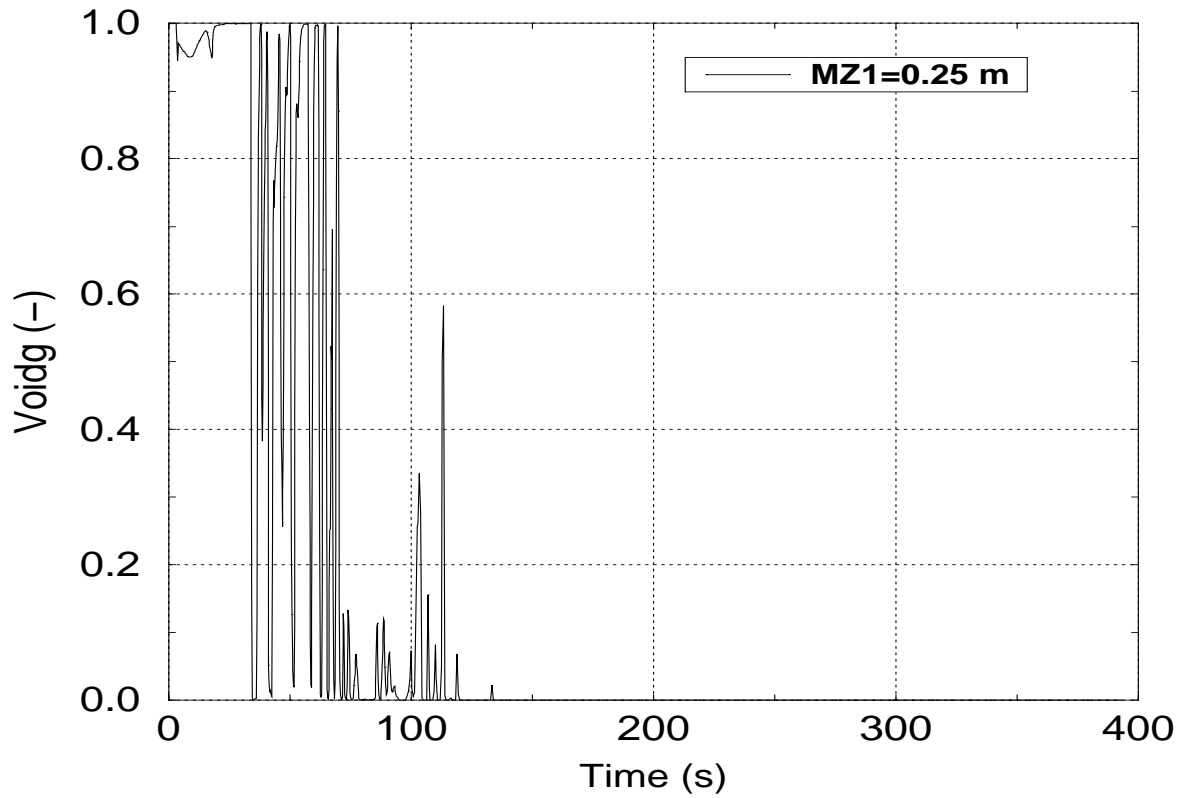


Figure 4-14 Predicted void fraction at core inlet

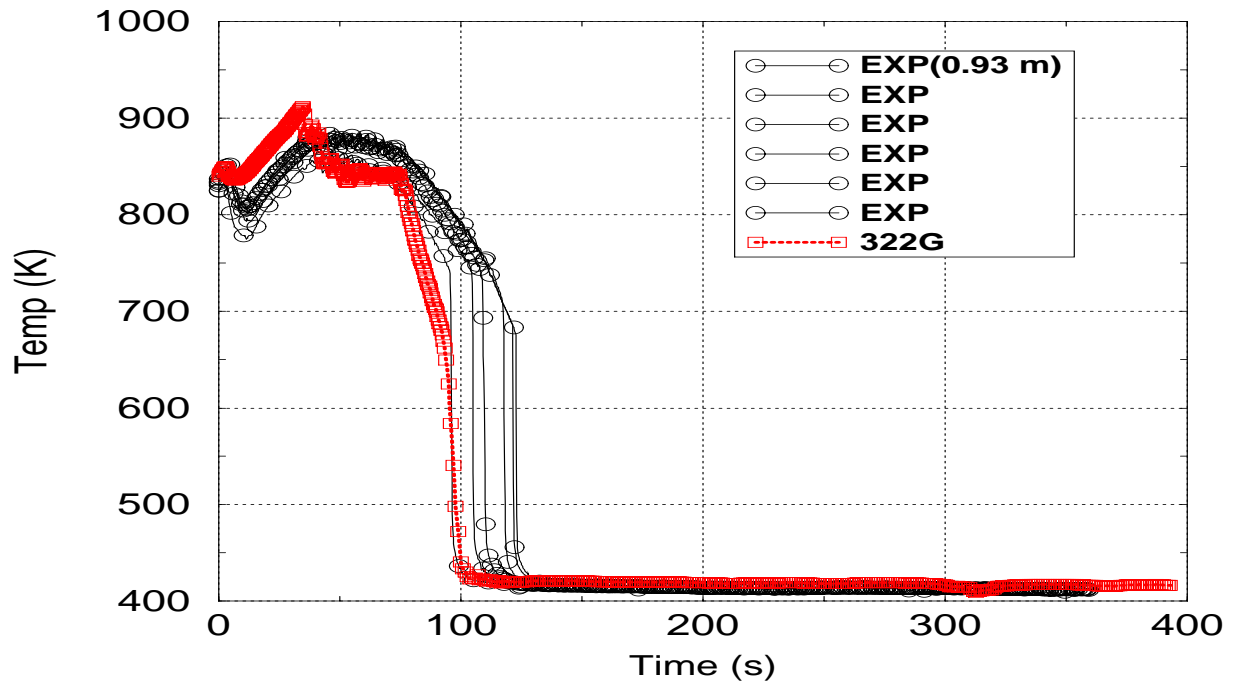


Figure 4-15 Comparison of predicted and measured cladding temperature

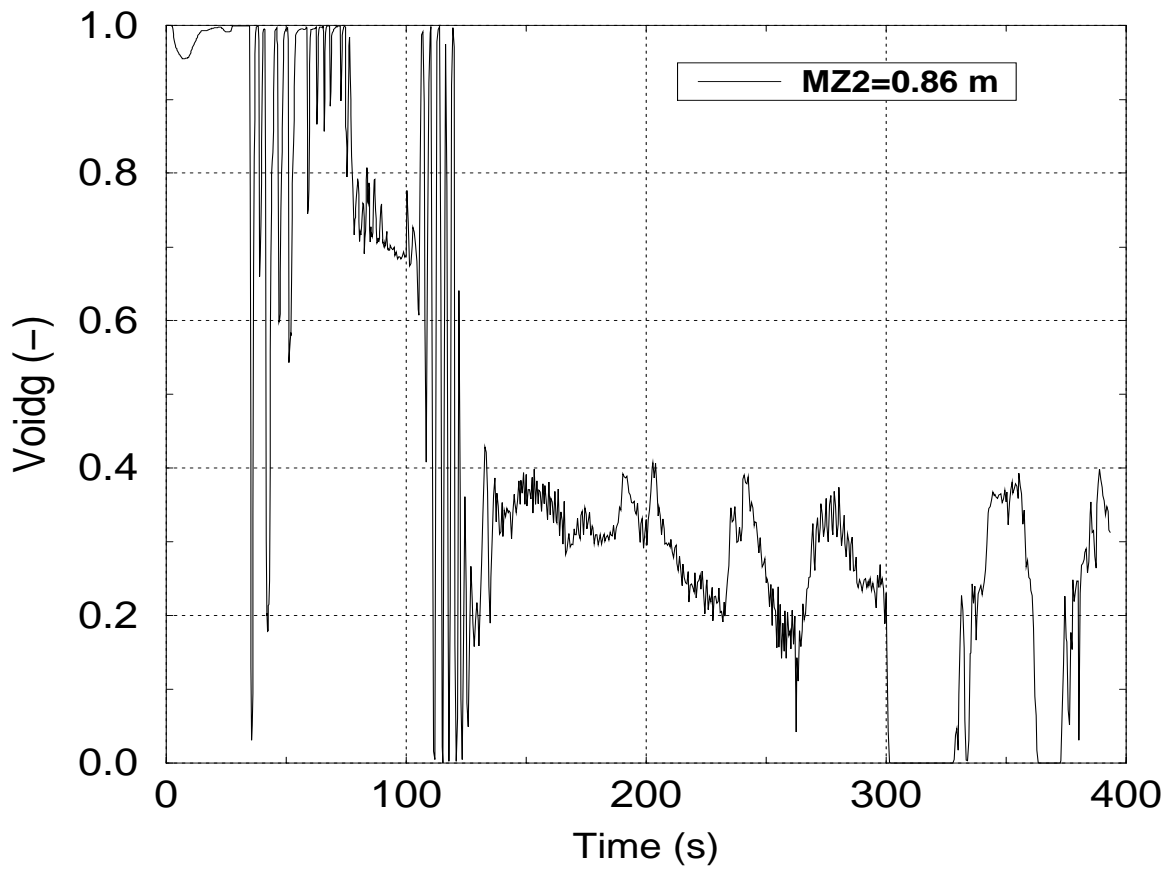


Figure 4-16 Predicted void fraction at 0.86 m elevation

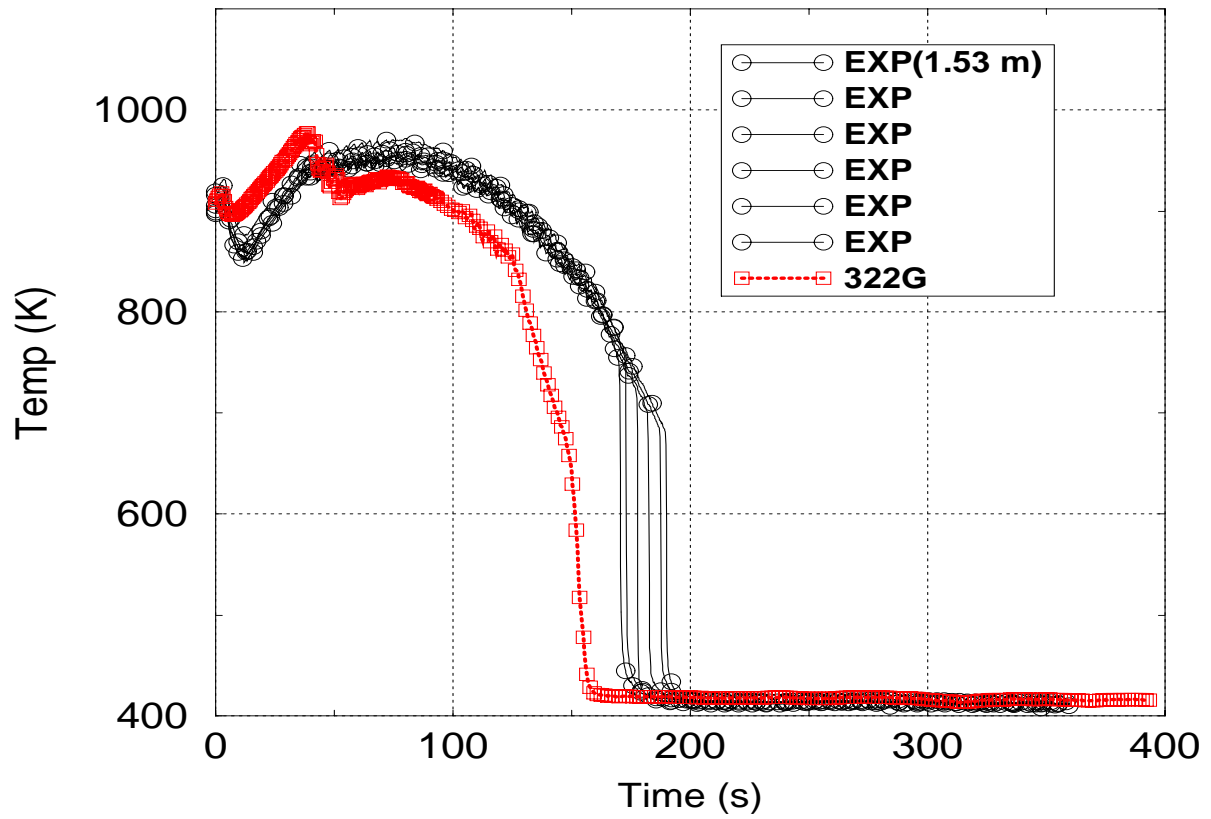


Figure 4-17 Comparison of predicted and measured cladding temperature

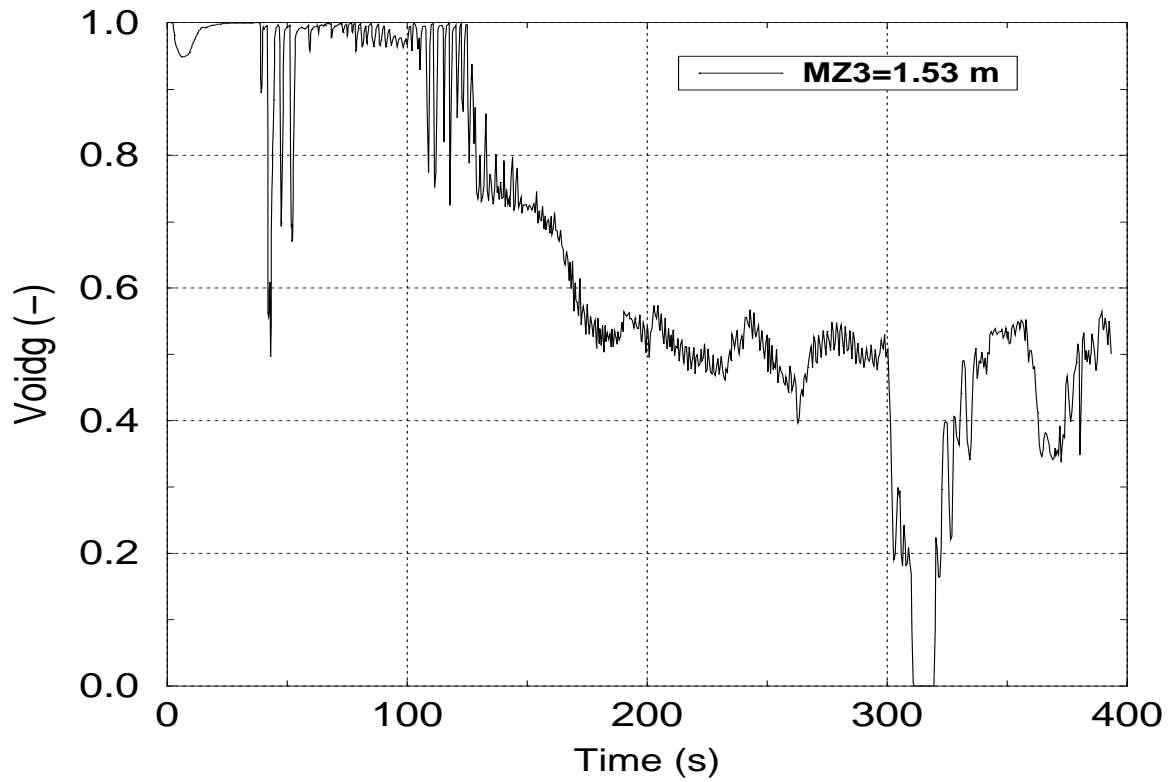


Figure 4-18 Predicted void fraction

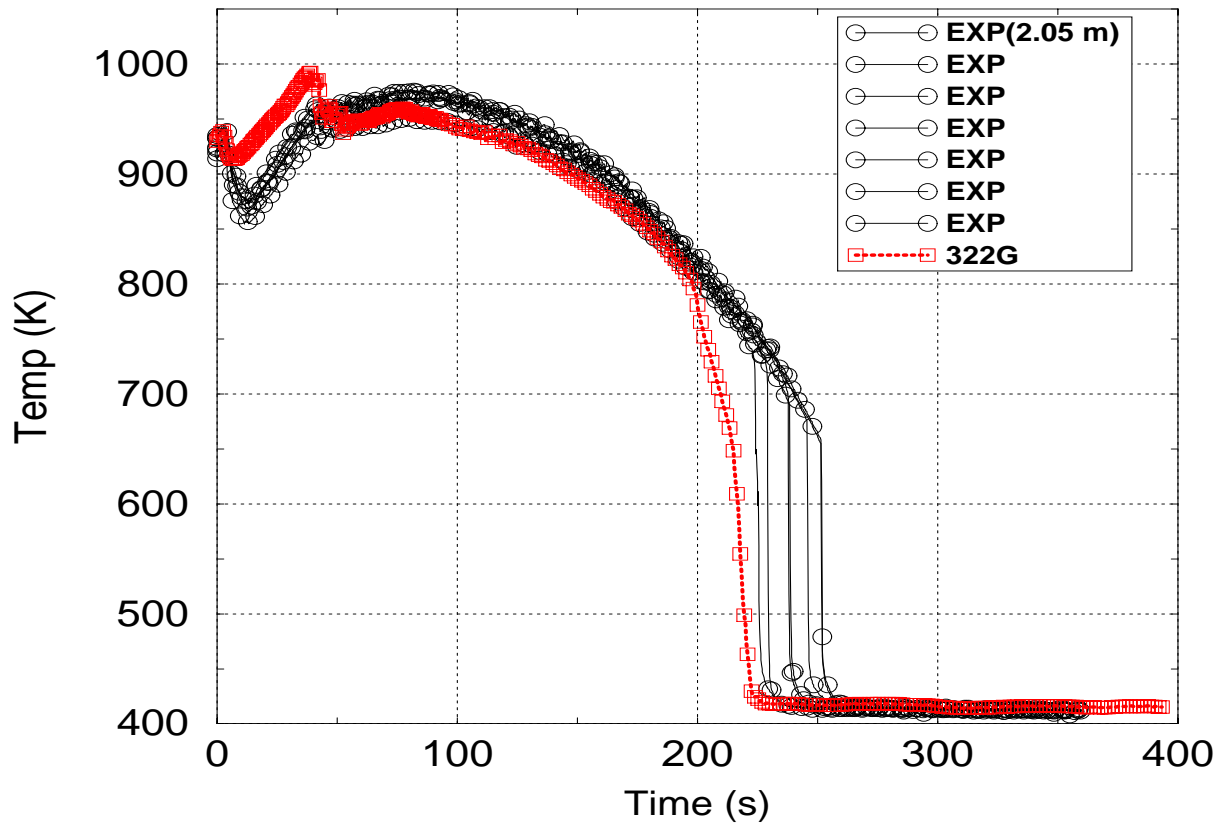


Figure 4-19 Comparison of predicted and measured cladding temperature

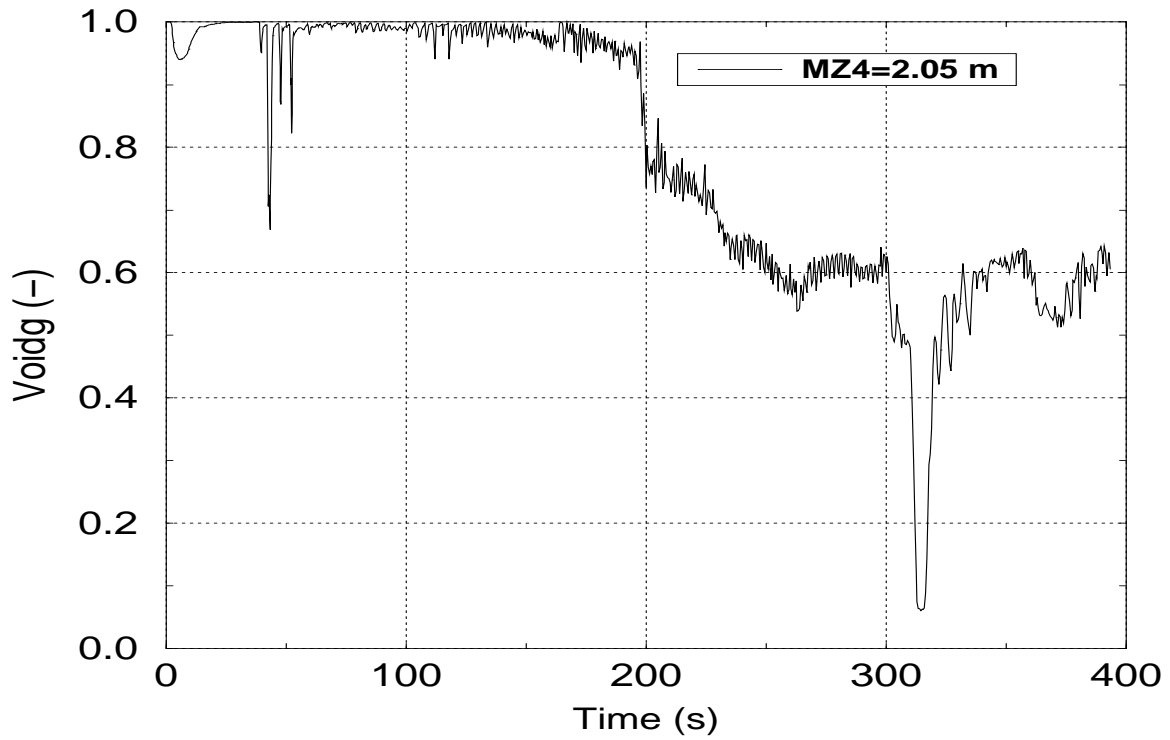


Figure 4-20 Predicted void fraction at 2.05 m elevation

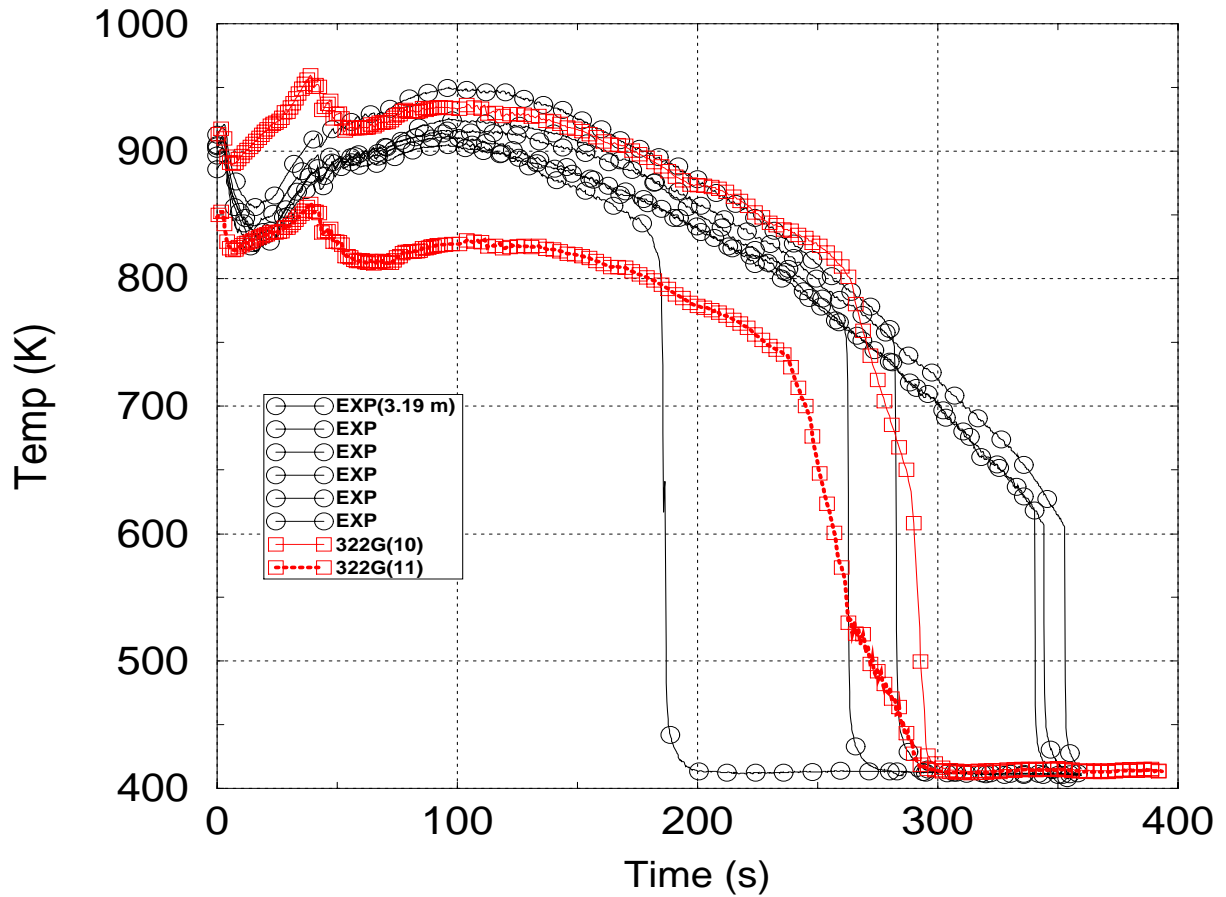


Figure 4-21 Comparison of predicted and measured cladding temperature

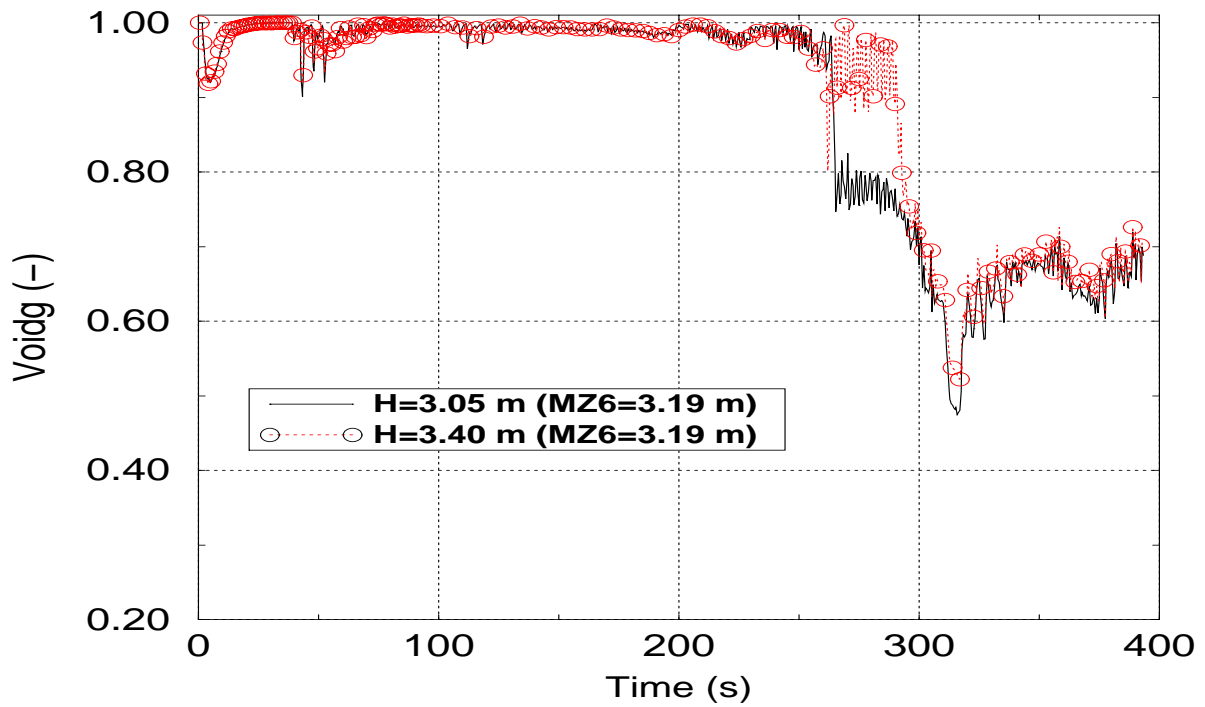


Figure 4-22 Predicted void fraction in two neighbour nodes

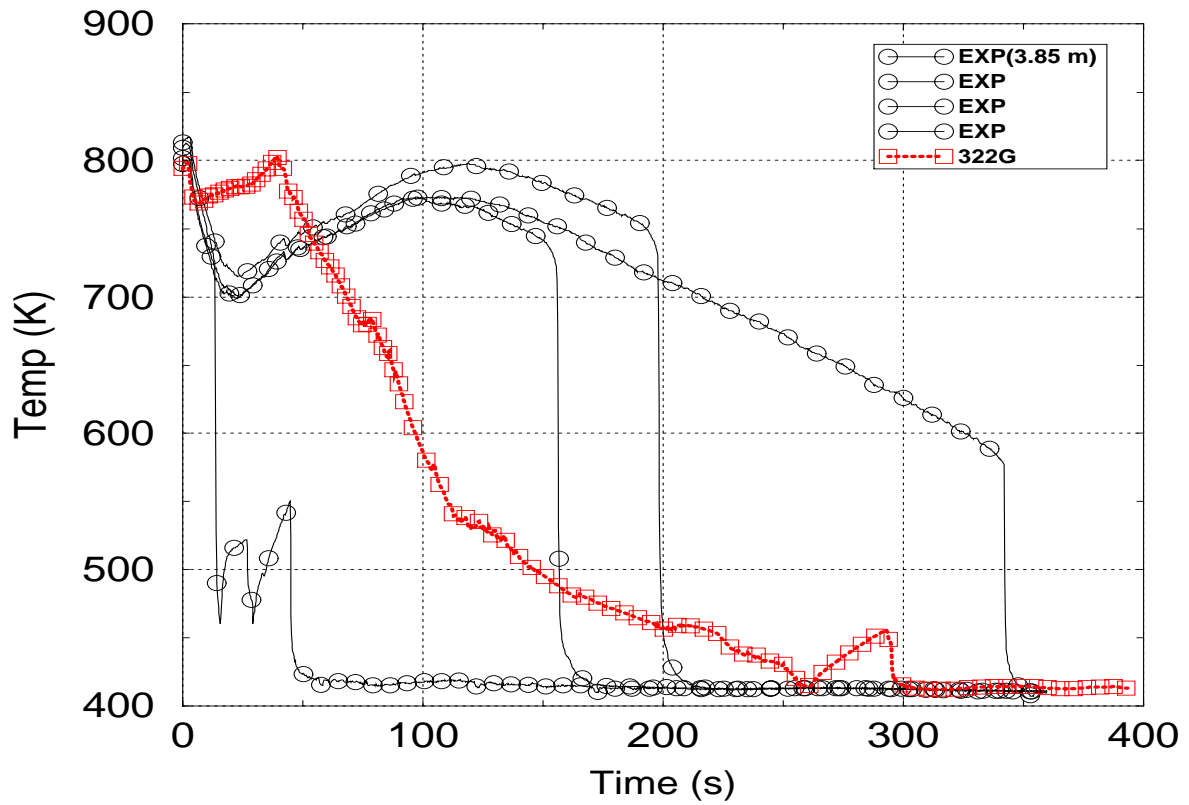


Figure 4-23 Comparison of predicted and measured cladding temperature

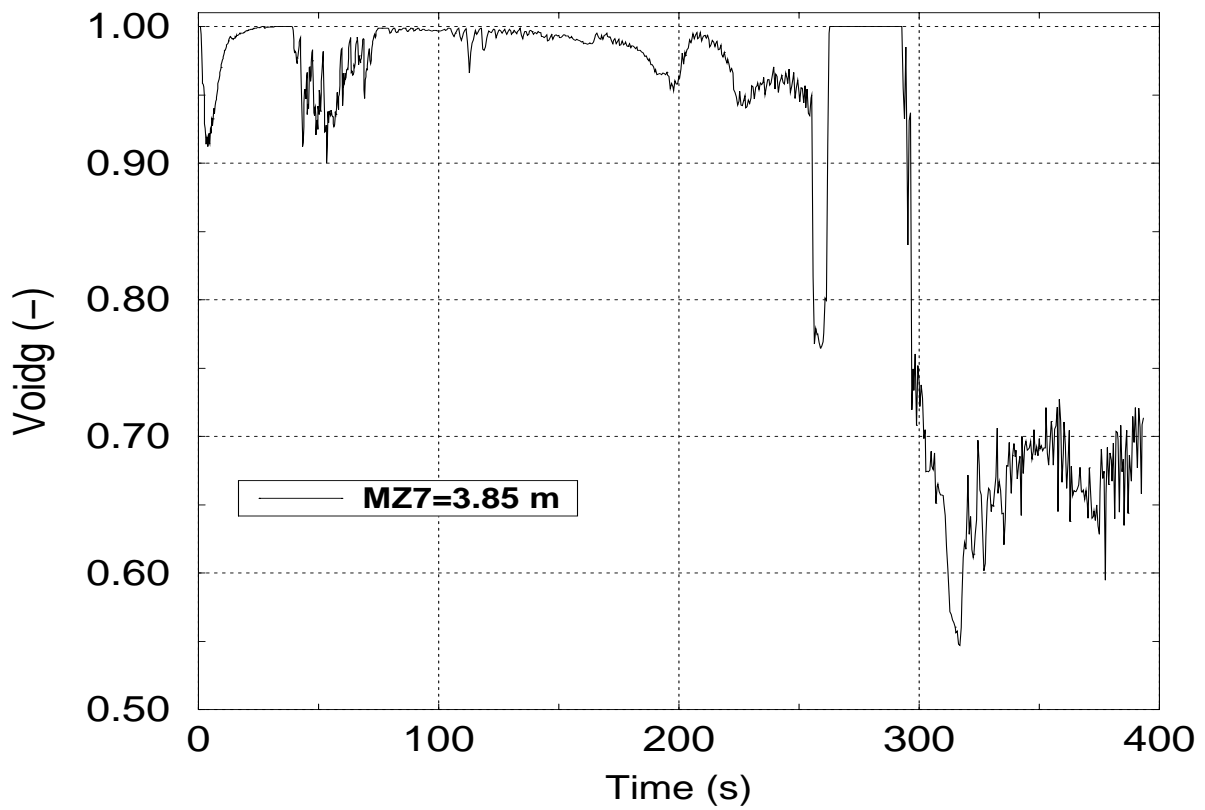


Figure 4-24 Predicted void fraction in two neighbour nodes

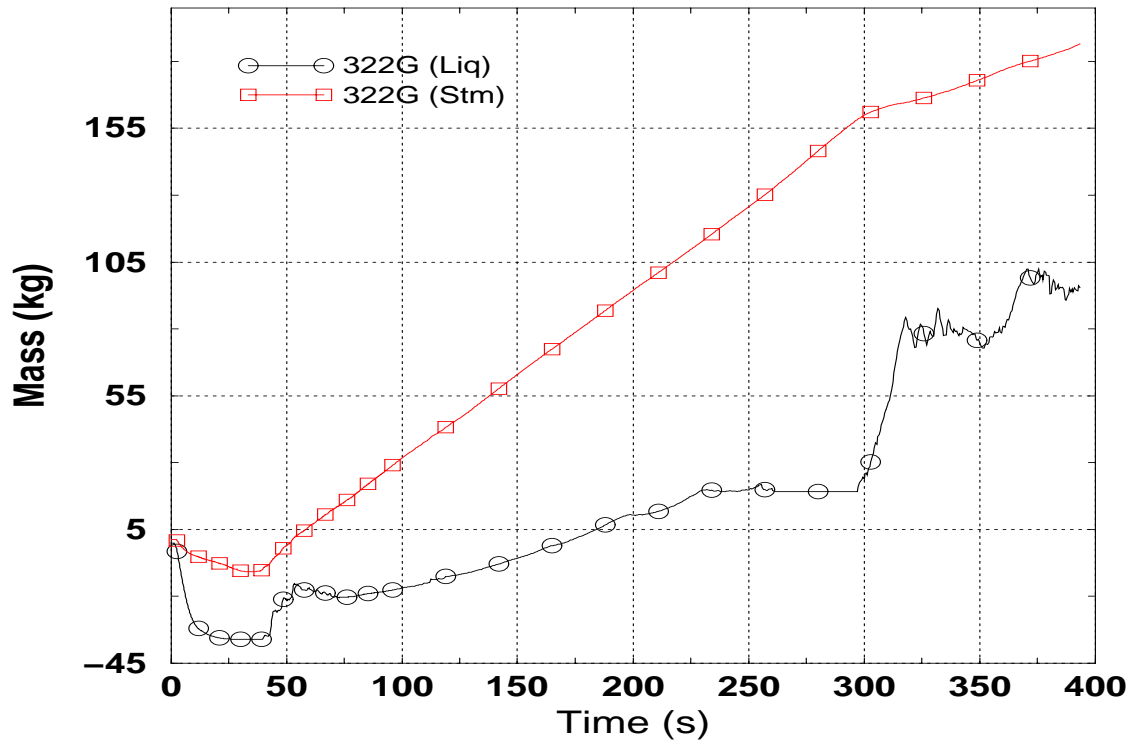


Figure 4-25 Predicted integral core outlet mass outflow

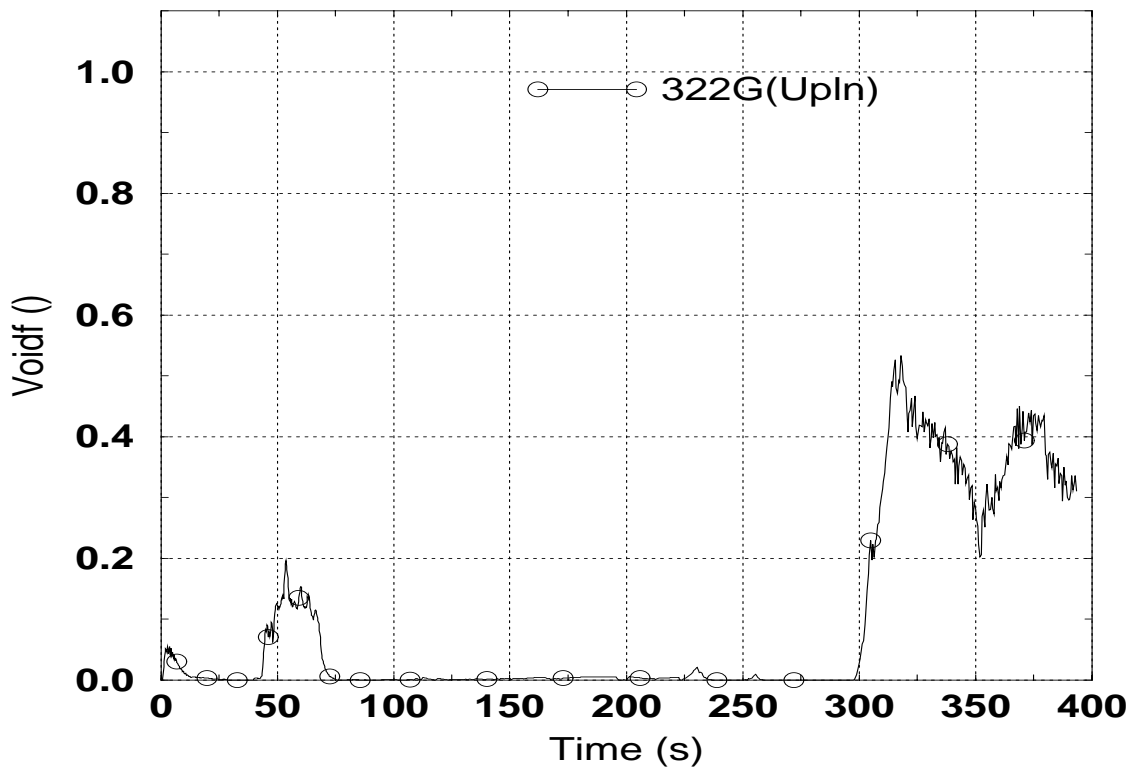


Figure 4-26 Predicted liquid void fraction in the upper plenum

4.2 Results with the modified version RELAP5/MOD3.2.2Gamma+FZK

The PKL IIB.5 test was recalculated with the improved version RELAP5/MOD3.2.2Gamma+FZK (322G+FZK), in which the Weisman correlation was replaced by the FZK-transition boiling model (see Appendix B). Good results has been obtained with this version 322G+FZK for the integral test LOFT-LP-LB-1 [Sanch01].

In Figure 4-27 to Figure 4-33 the cladding temperature predicted by both the original 322G-version and the improved 322G+FZK-version is compared with the data for selected bundle elevations. It can be seen that the predictions of both code versions are close to each other in almost all elevations, except for the upper bundle part. Even in the lower and middle elevations the differences in the temperature are mainly related to the dispersed and transition boiling heat transfer and specially to the rewetting temperature. In the upper most elevation, Figure 4-33, the overall temperature trend predicted by 322G+FZK is very close to the data while the one of the 322G-version considerably diverges from data.

From the comparison of both predictions it can be stated that the FZK-transition boiling model predicts a higher quench temperature that is closer to experimental findings than the Weisman correlation. In Figure 4-34, Figure 4-35, and Figure 4-36 a comparison of the predicted rewetting temperature with the data is given for the time around the quench time. The “knee-point” in the temperature curves marking the rewetting can be clearly seen. This knee-temperature is predicted much closer to the measurement values by the improved version 322G+FZK than by the original one. This results confirm the ones obtained for the LOFT-LP-LB-1 test, [Sanch01].

Due to the different transition boiling correlations of both code versions the heat transfer coefficient and the void fraction profile at different bundle elevations are qualitatively but not quantitatively similar. These parameters and the heat transfer mode are depicted in Figure 4-37, Figure 4-38, and Figure 4-39. The differences between both predictions increase at higher elevations. For example at 3.85 m elevation, the heat transfer coefficient predicted by 322G shows two peaks, the first one very early in time, Figure 4-40, Figure 4-41, and Figure 4-42 while the one predicted by 322G+FZK has only one peak. In addition the void fraction predicted by the original 322G-version shows a more oscillatory behaviour than the 322G+FZK-version.

It has to be noted that at the uppermost elevation the Weisman-correlation does not predict a quench-like clad temperature behaviour. Instead a continuous cooling of the rod segment at the elevation is predicted, Figure 4-33.

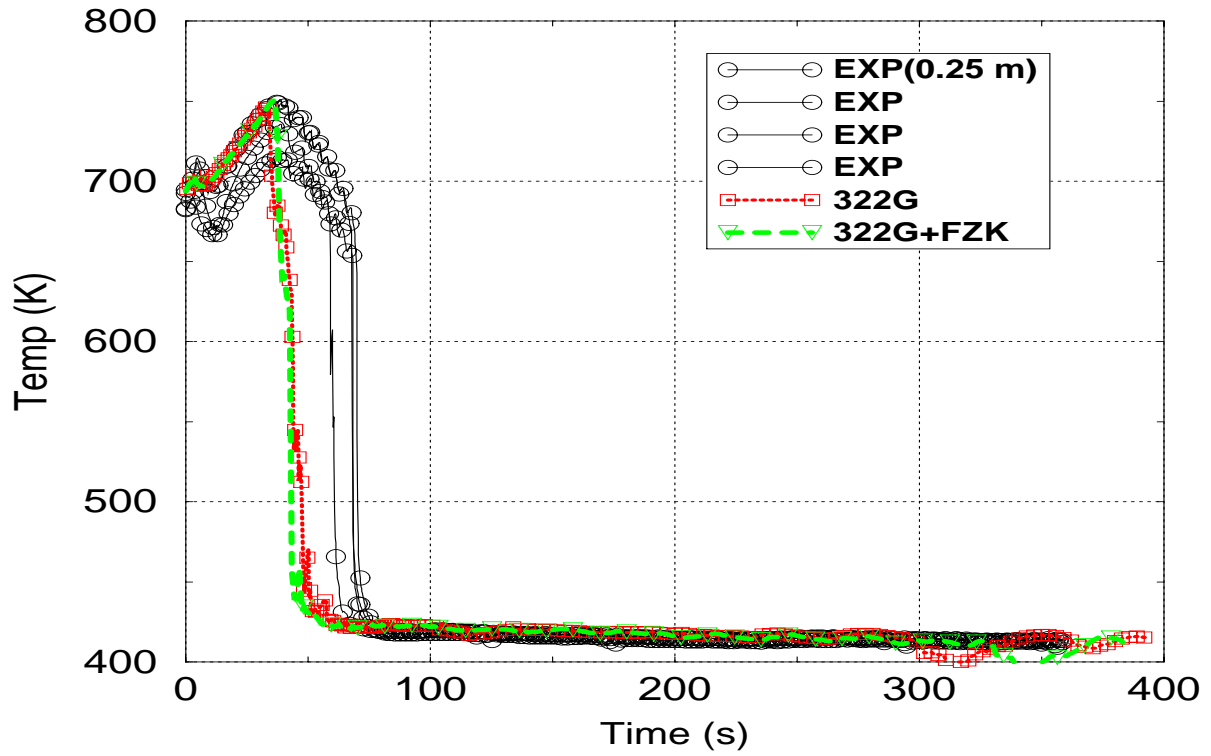


Figure 4-27 Comparison of RELAP5-predictions with data

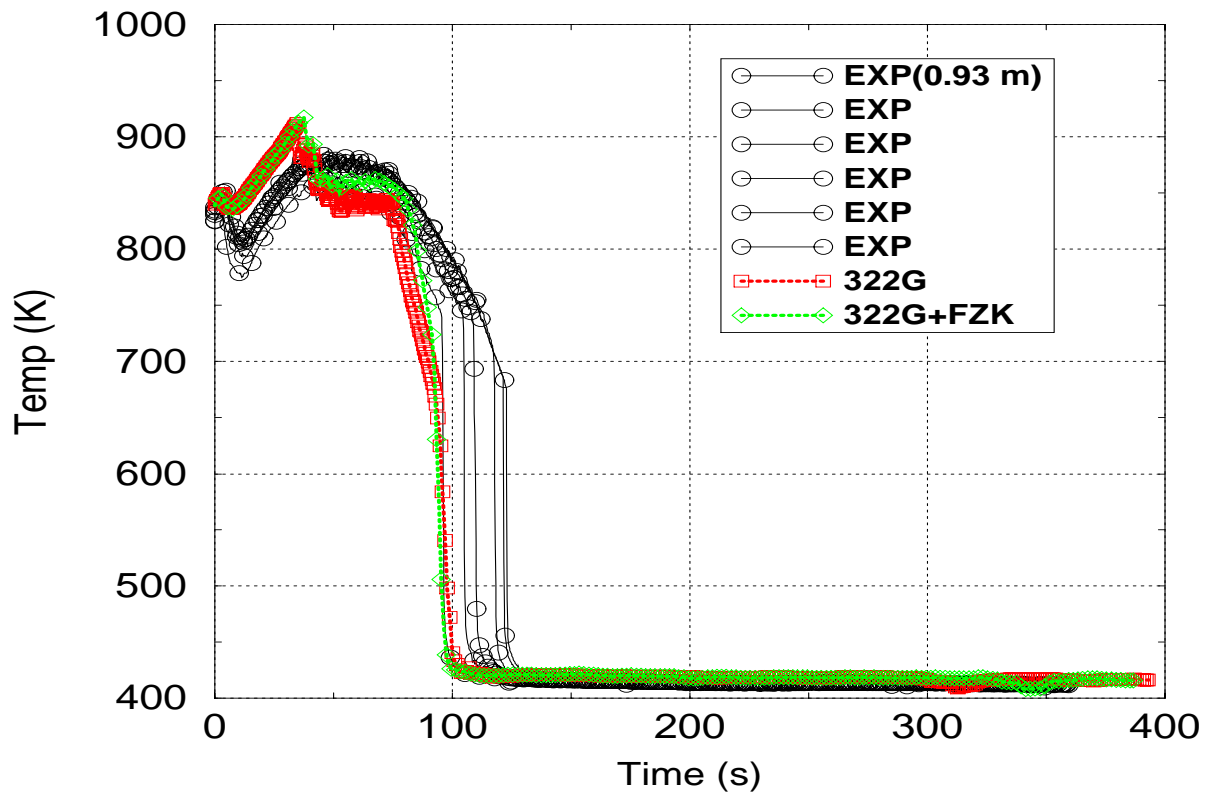


Figure 4-28 Comparison of RELAP5-predictions with data

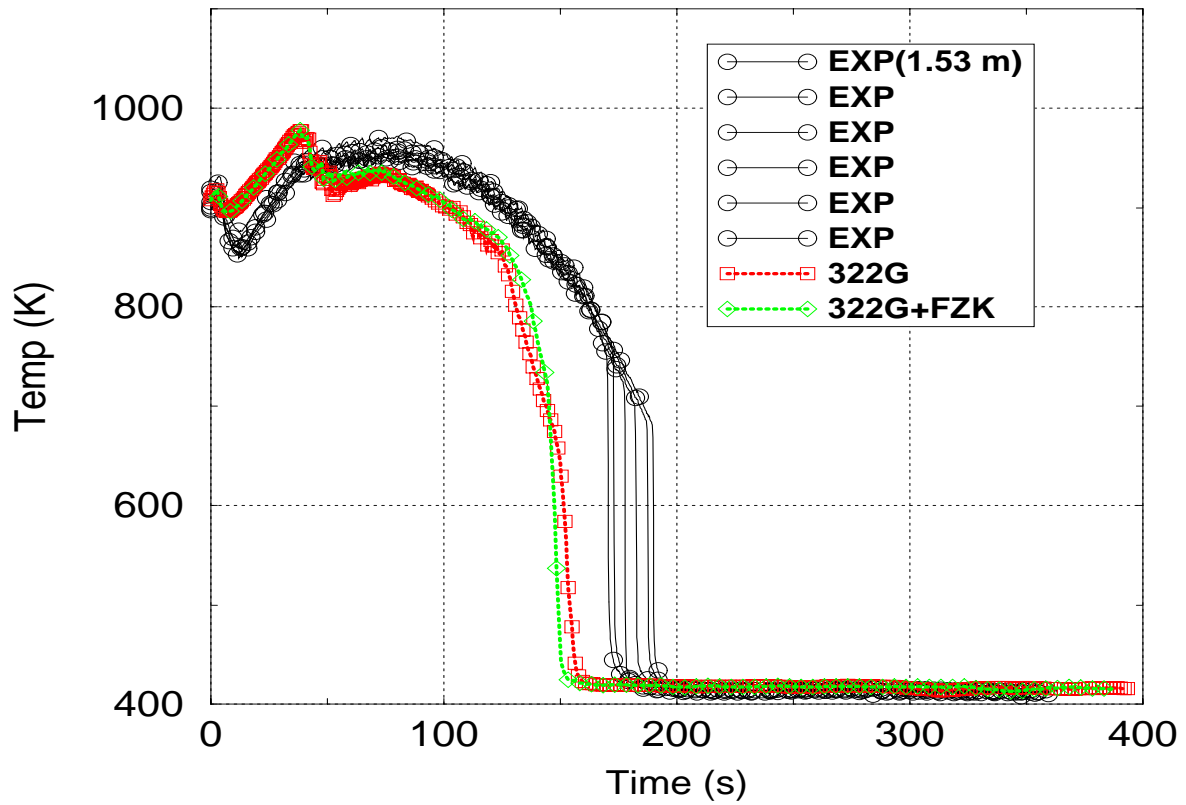


Figure 4-29 Comparison of RELAP5-predictions with data

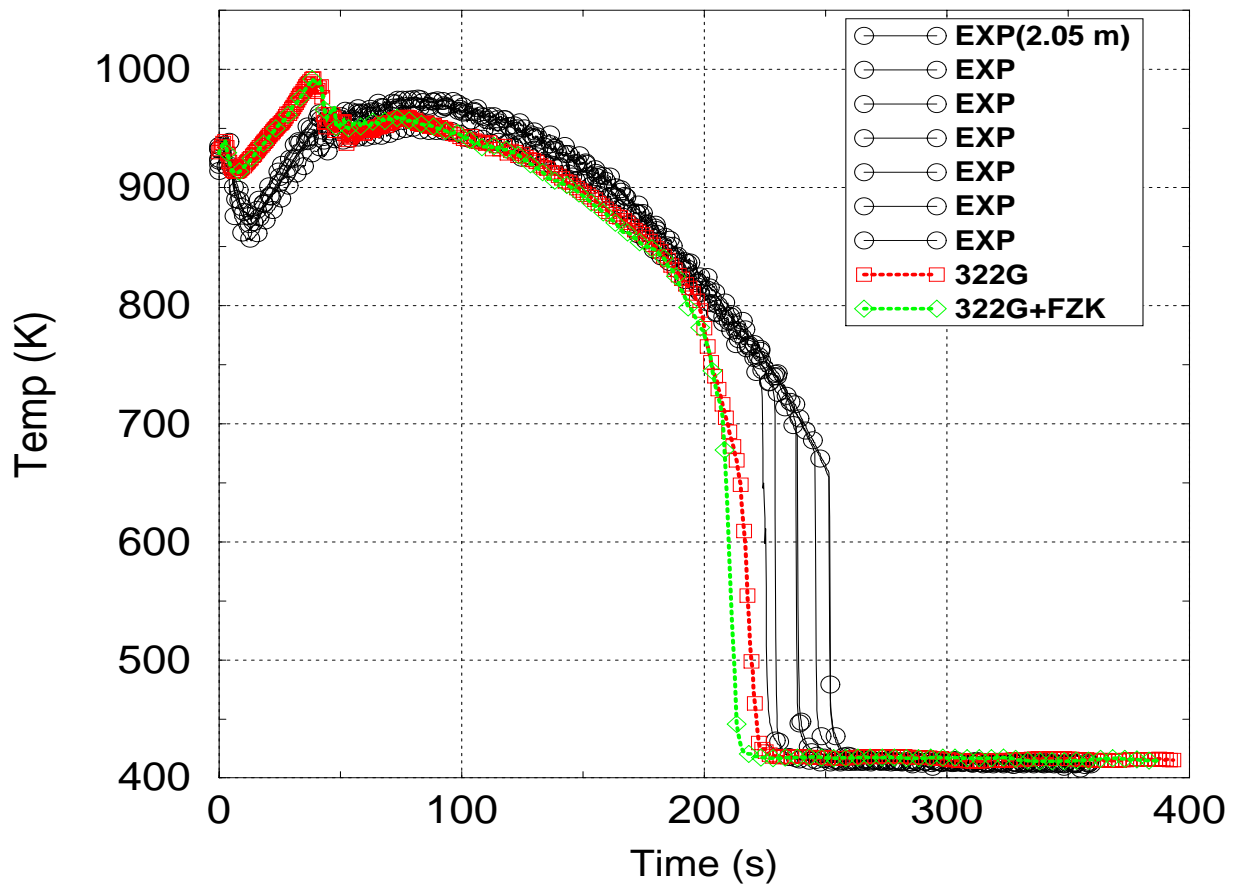


Figure 4-30 Comparison of RELAP5-predictions with data

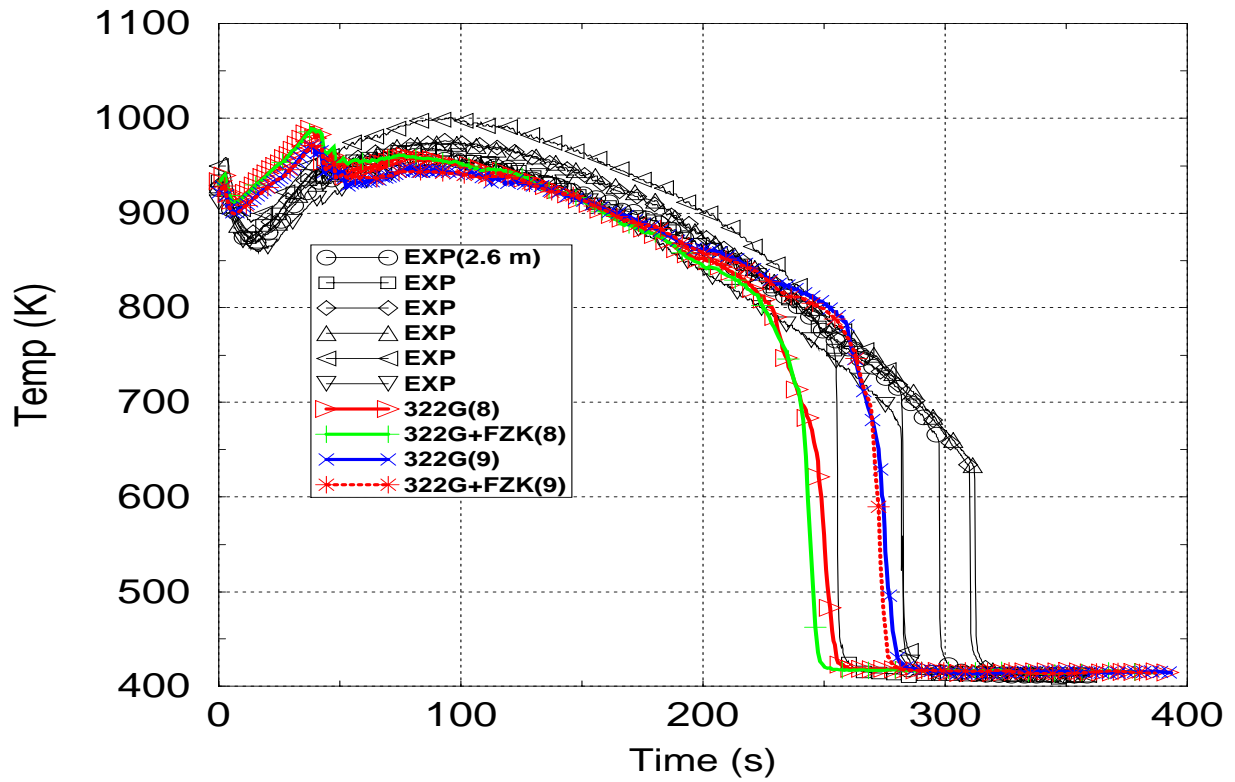


Figure 4-31 Comparison of RELAP5-predictions with data

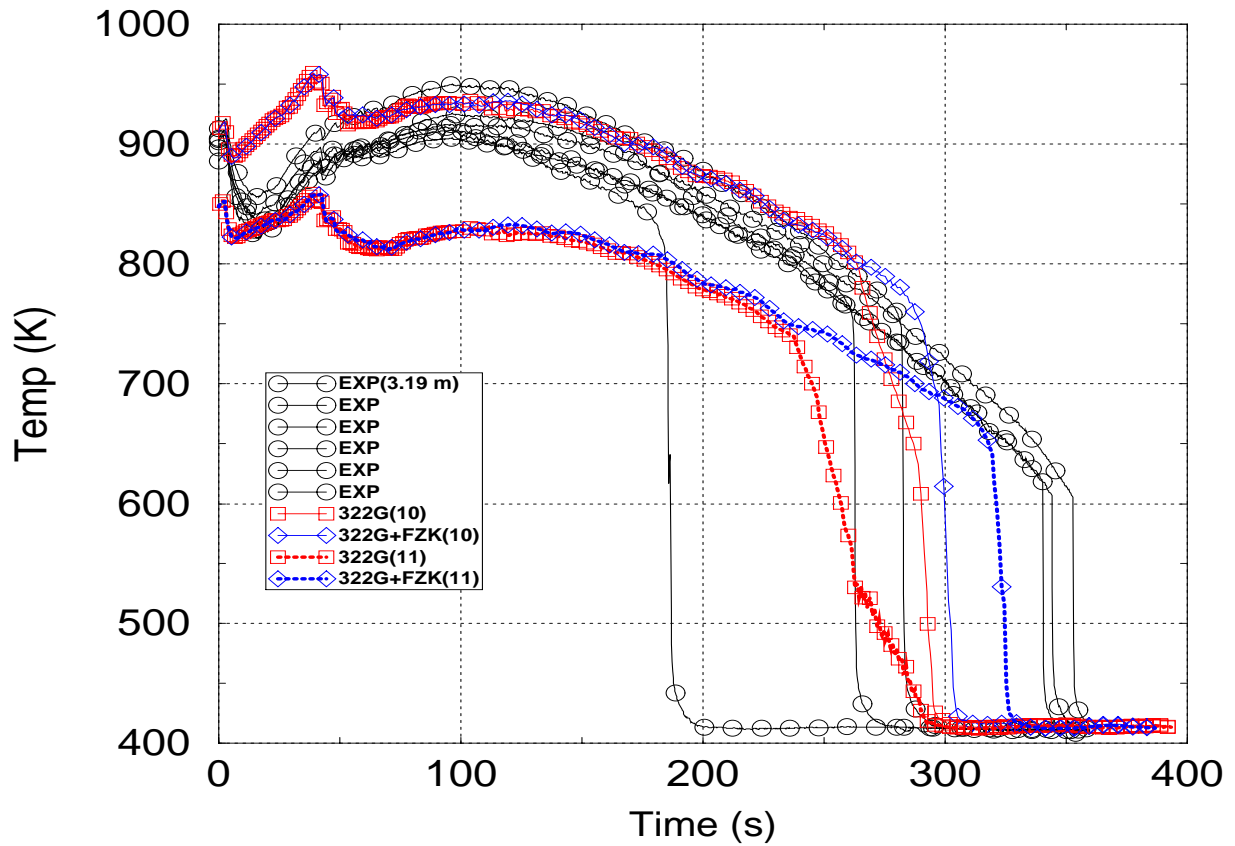


Figure 4-32 Comparison of RELAP5-predictions with data

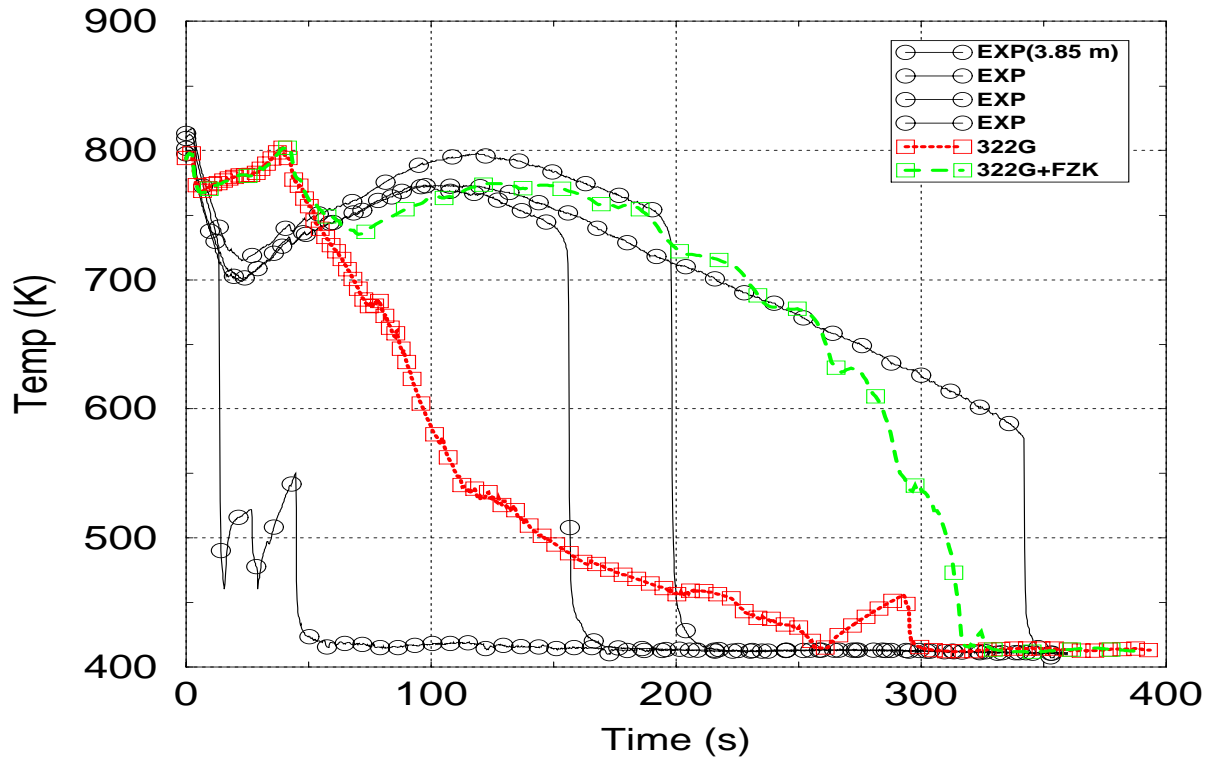


Figure 4-33 Comparison of RELAP5-predictions with data

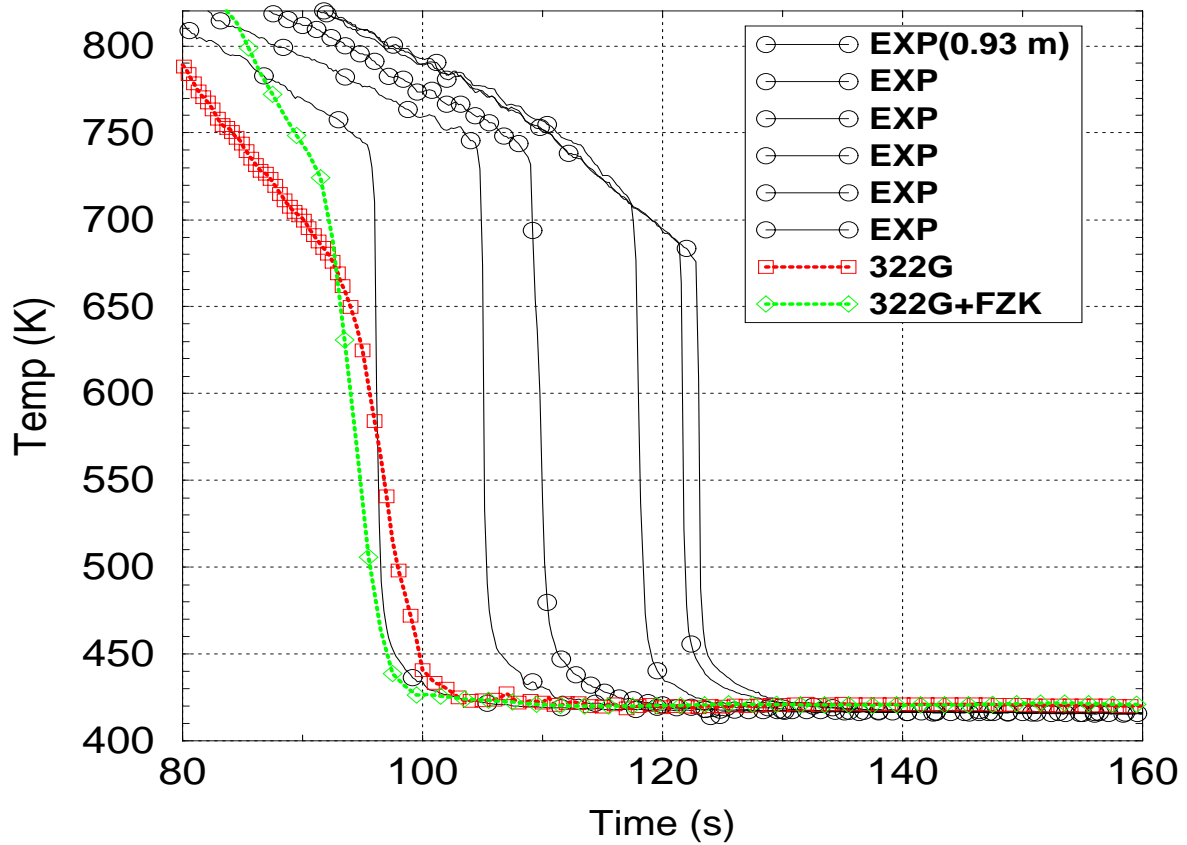


Figure 4-34 Comparison of predicted and measured rewetting temperature

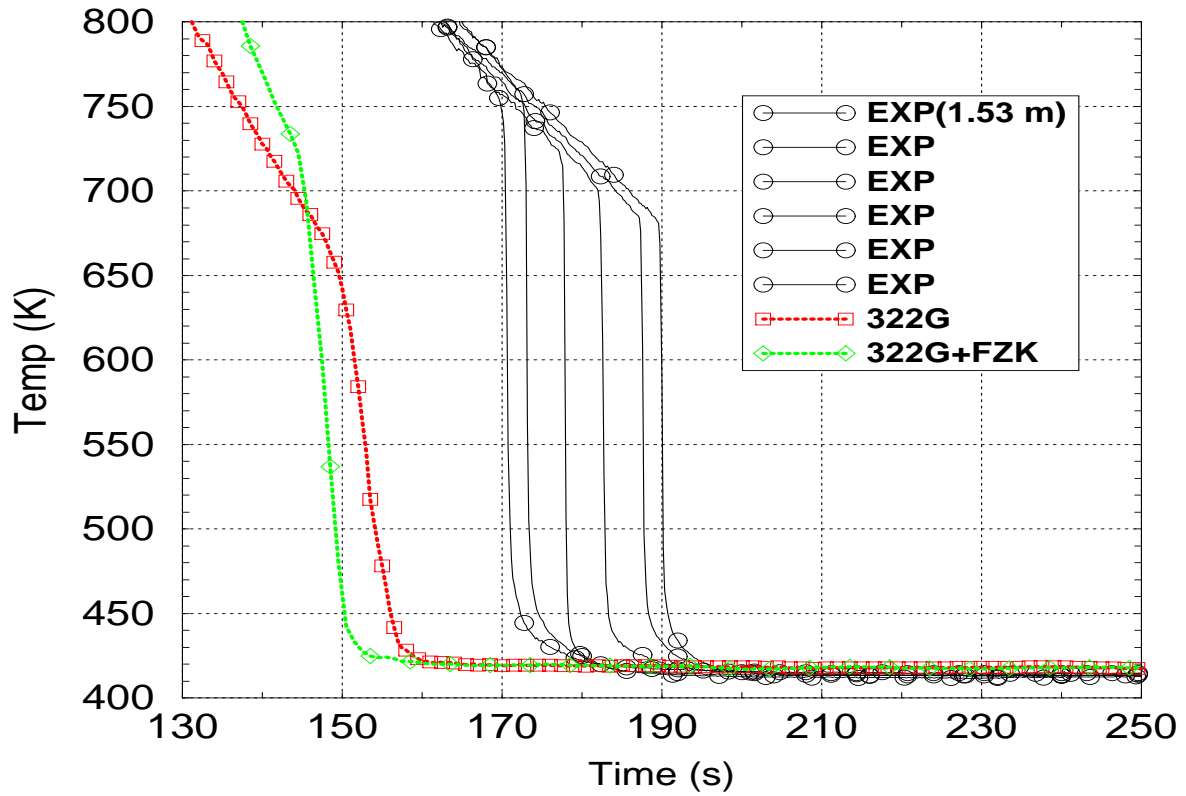


Figure 4-35 Comparison of predicted and measured rewetting temperature

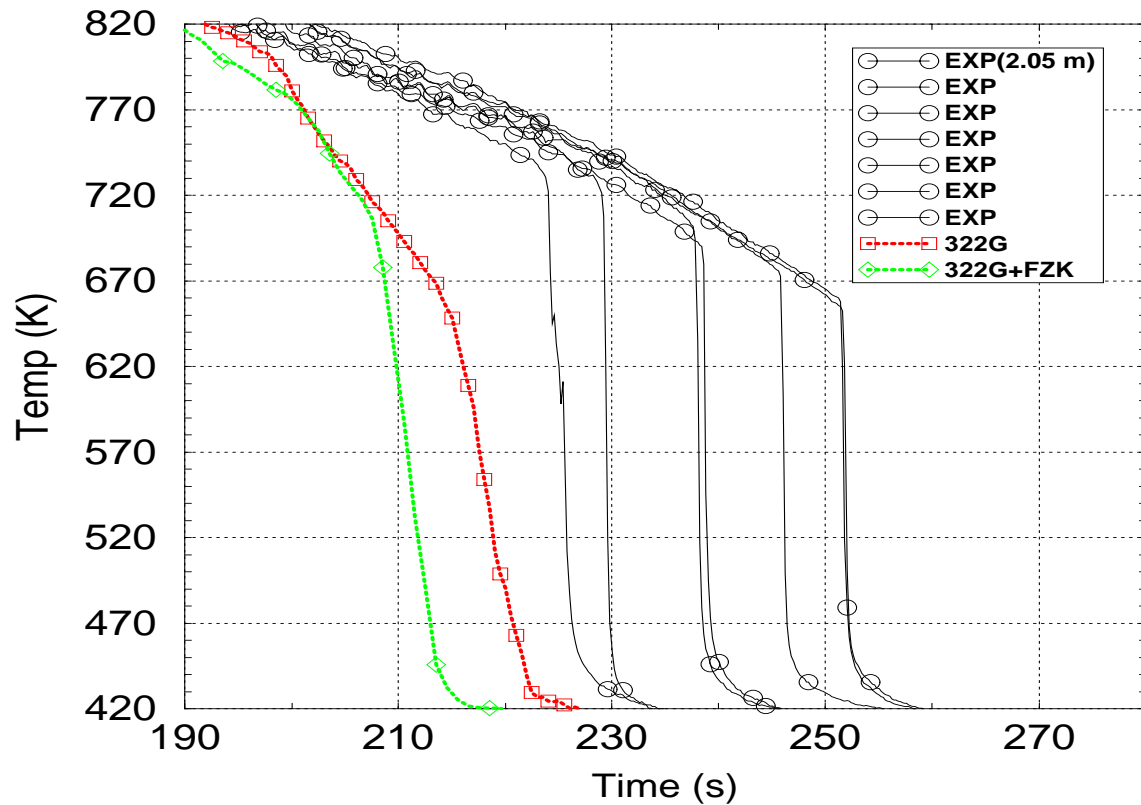


Figure 4-36 Comparison of predicted and measured rewetting temperature

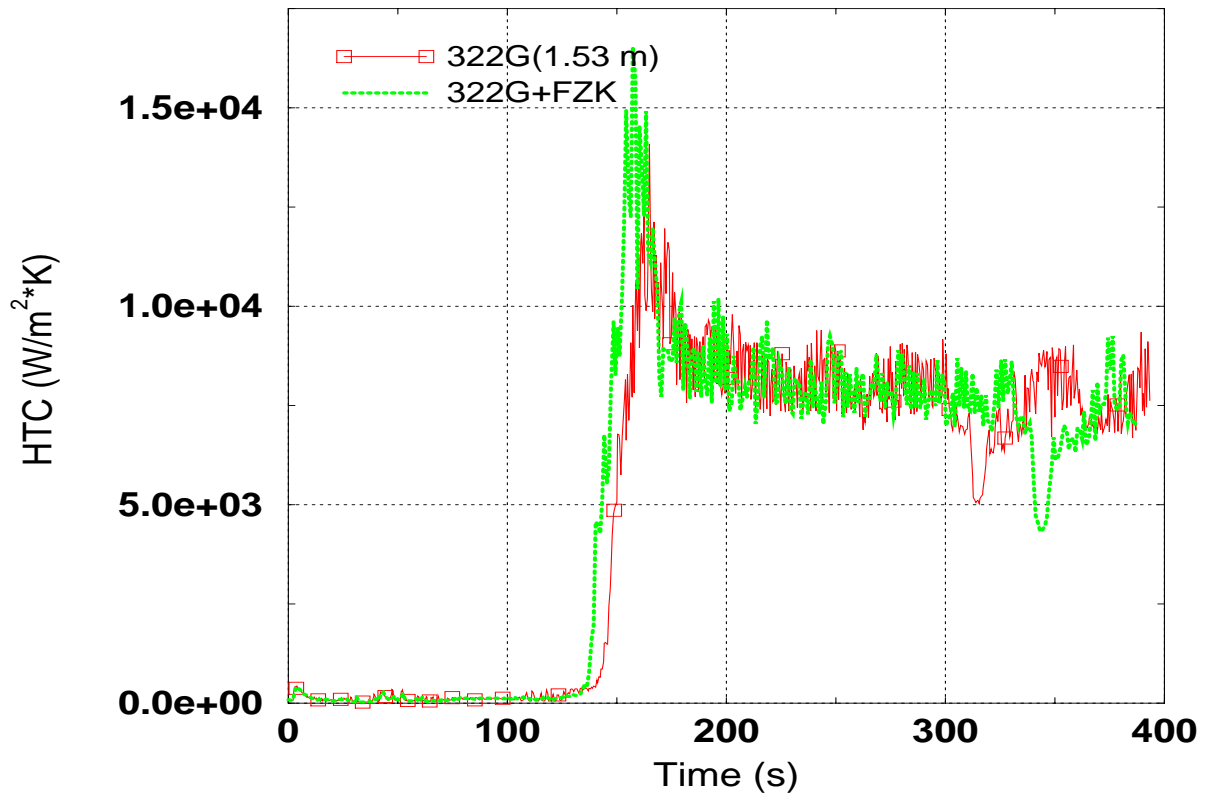


Figure 4-37 Predicted heat transfer coefficient at 1.53 m core elevation

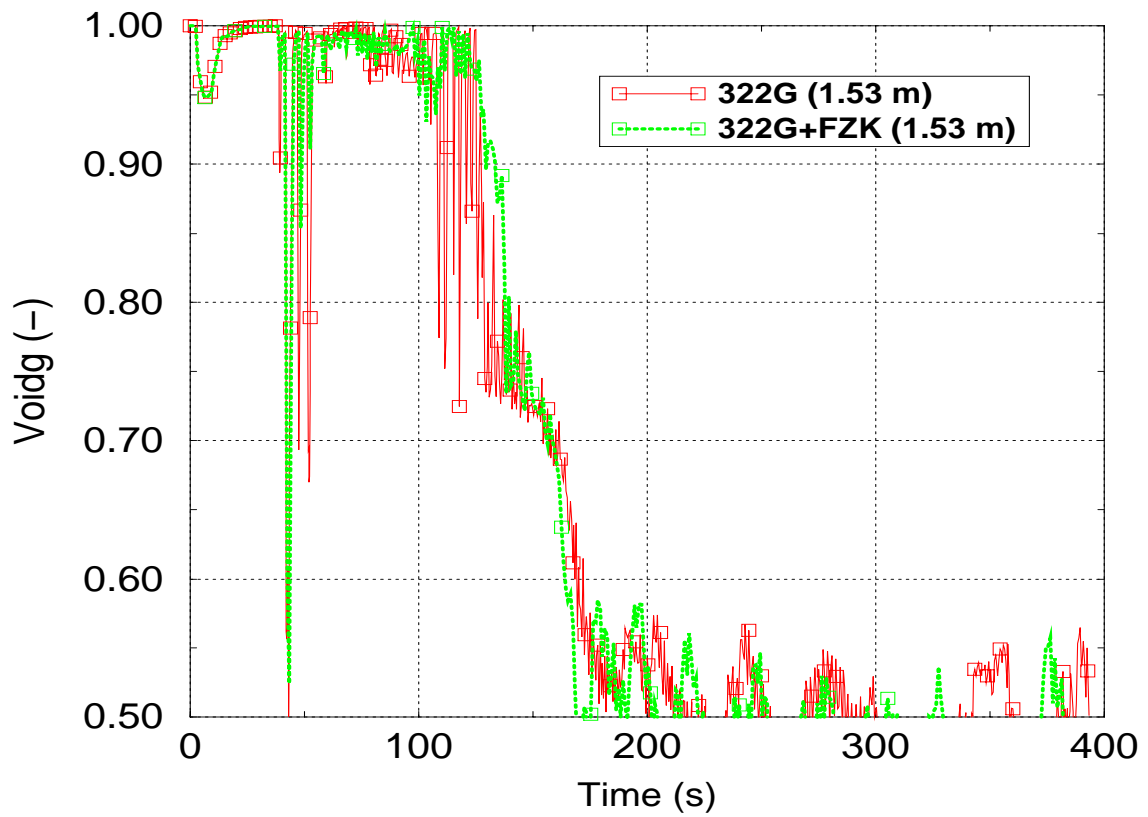


Figure 4-38 Predicted void fraction at 1.53 m core elevation

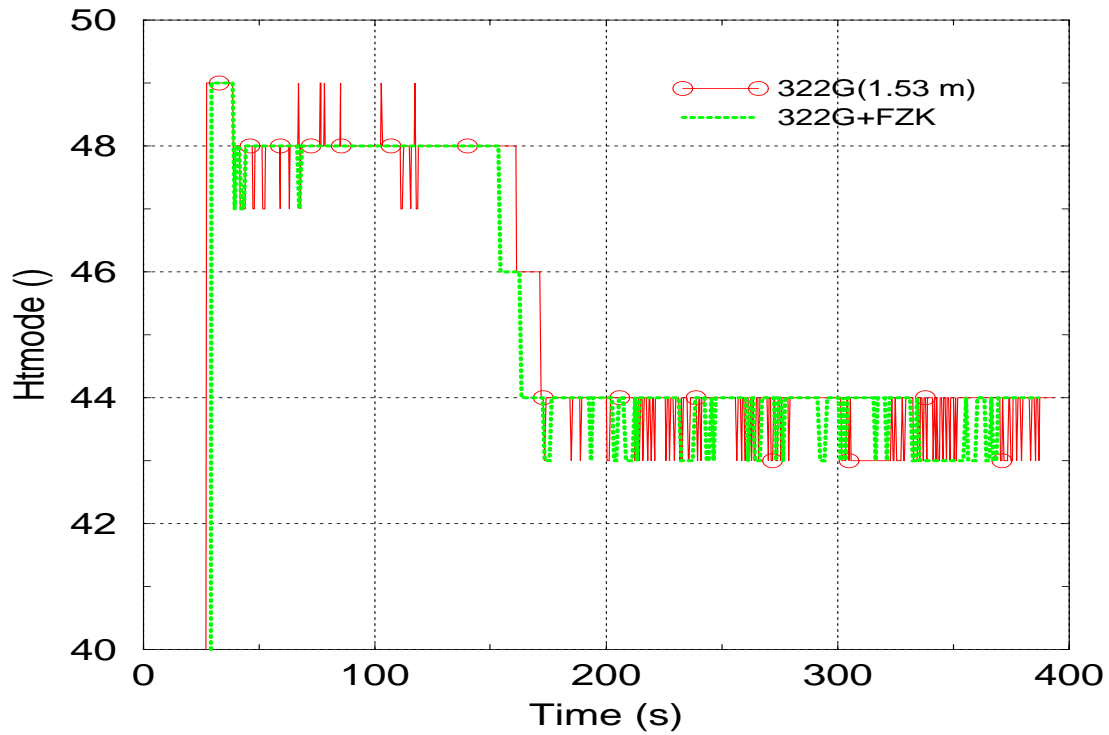


Figure 4-39 Predicted heat transfer mode at 1.53 m core elevation

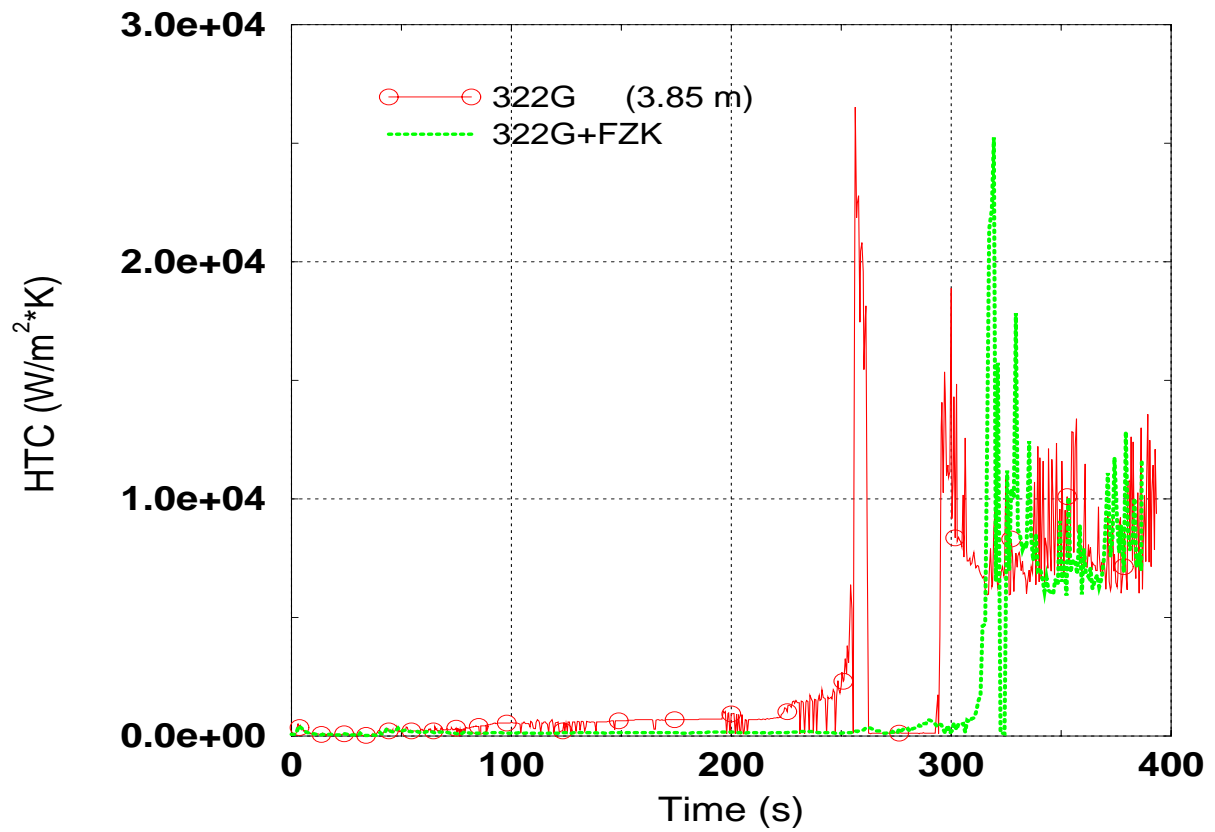


Figure 4-40 Predicted heat transfer coefficient at 3.85 m core elevation

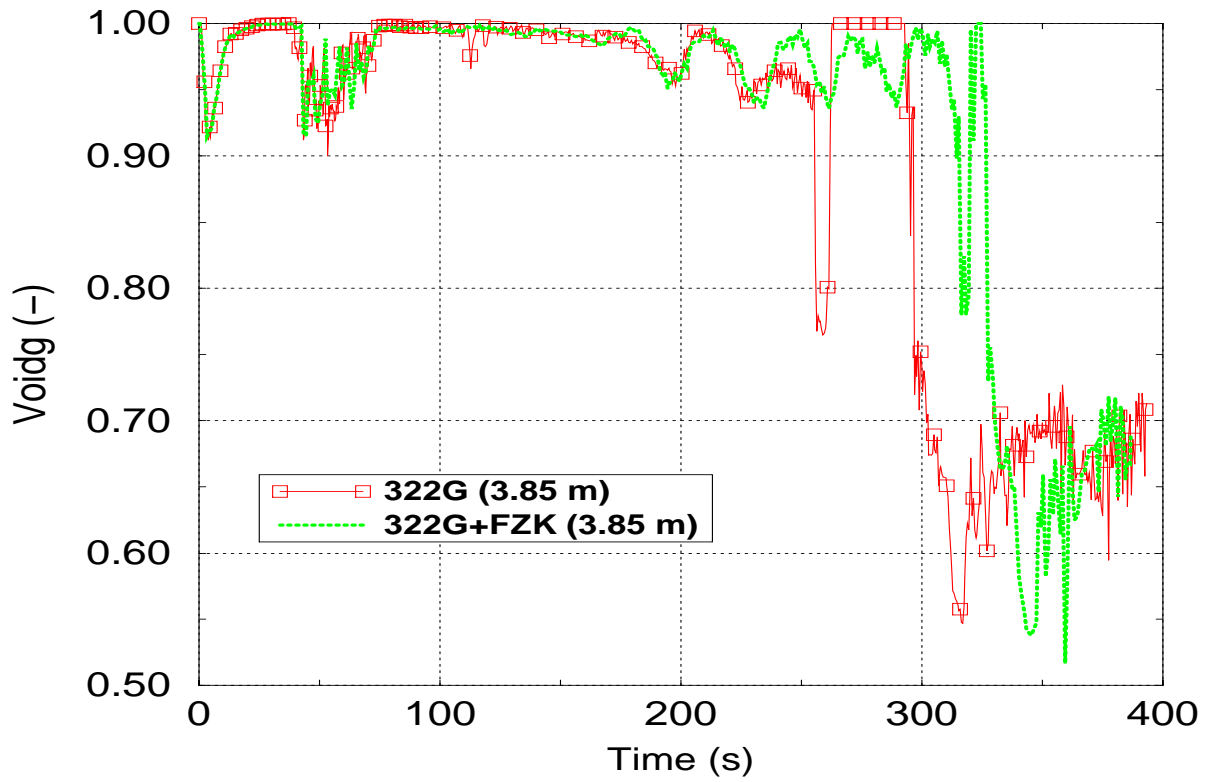


Figure 4-41 Predicted void fraction at 3.85 m core elevation

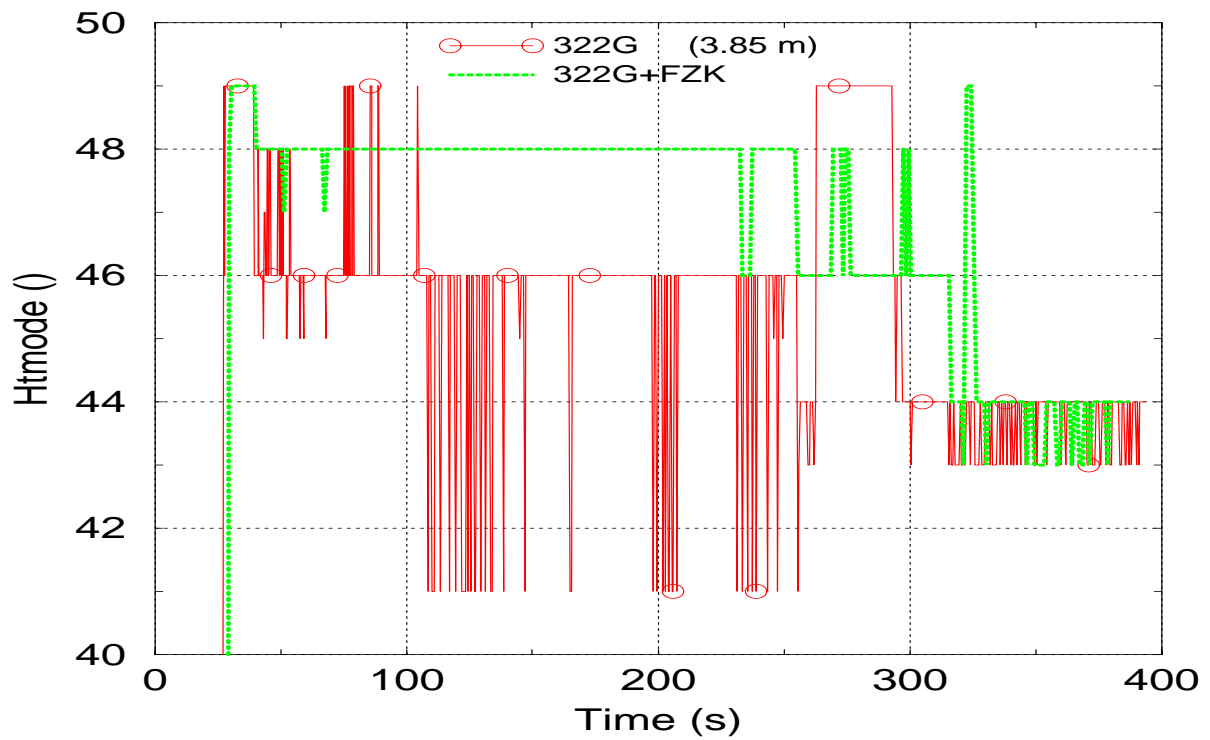


Figure 4-42 Predicted heat transfer mode at 3.85 m core elevation

5 Summary and conclusions

As part of the RELAP5 assessment work performed within the CAMP-Program at FZK different RELAP5-code versions have been validated using reflood data obtained by single rod, bundle, and integral experiments.

The post-test calculations were carried out with two RELAP5-versions, the original (R5M322G) and the improved one (R5M322G+FZK) using a PKL-model developed by Siemens/KWU for an older RELAP5-version. This model was modified by FZK to appropriately meet test initial conditions of PKL-IIB.5.

Based on post-test calculations of the PKL-test using the original version R5M322G it can be concluded that the RELAP5-predictions are qualitatively in good agreement with the measured cladding temperature trends in almost all elevations except the uppermost one. There no quench-like cool-down of the bundle segment was predicted by the code. Based on these results it can be stated that the PSI-reflood model predicts the overall reflood heat transfer mechanisms in a reasonable manner. Specially in the dispersed film boiling flow regime, where the highest fuel rod temperature were both measured and calculated, a very good agreement between predictions and measurement was encountered. This demonstrates the RELAP5 capabilities to predict important safety parameters like the maximal cladding temperature in a reliable manner. However it was noted that the Weisman-correlation tends to under-predict the rewetting temperature.

A re-evaluation of the PKL-IIB.5 test with the code version R5M322G+FZK, where the FZK-transition boiling model is implemented instead of the Weisman one, showed that the predicted rewetting temperature was closer to the data and thereby higher than the one predicted by 322G. This reconfirms the results obtained for LOFT-LP-LB-1 with the 322G+FZK-version.

Aside from the good results obtained with the PSI-reflood model some discrepancies between data and predictions still remain, especially downstream of the quench front, when the entrainment of droplets is considerable. Under such conditions the heat transfer between phases, e.g. droplets and continuous vapour plays an important role and needs to be taken into account by more mechanistic models.

6 Future work

Despite the considerable progress in modelling the reflood heat transfer, e.g. within RELAP5, additional experimental investigations are still necessary to fully understand the fundamental mechanisms governing the reflood heat transfer. Further model improvements may be feasible with the implementation of mechanistic models in RELAP5 that treat the droplets and its interaction with the continuous vapour phase in a more realistic manner [Rose99]. Hence attention will be focused on the following areas: 1) use of findings from experimental investigation being performed on the RBHT-facility at the PSU, and 2) Check applicability of current models on high-temperature quenching situations using data from FZK QUENCH test program.

7 Literature

- [Anal96] G. T. Analytis; Developmental assessment of RELAP5/MOD3.1 with the separate-effect and integral experiments: Model changes and options. PSI Ber.96-09. Paul Scherrer Institut, Switzerland, April 1996.
- [Anal99] G. T. Analytis; Resolution of user problem NRCUPN1998559 and mass error suppression in PANDA calculations with RELAP5/MOD3.2.2Beta, TM-42-99-13, May. 1999.
- [Ban99] Ban, Chan-Han, W. Hering; Assessment of RELAP5 Reflood Model using PKL-II B5 test. PSF-Report.3322. March 1999.
- [Besti96a] D. Bestion, F. Barré, B. Faydide. Methodology, Status and Plans for Development and Assessment of the CATHARE Code. OECD/CSNI Workshop on Transient Thermalhydraulic and Neutronic Code Requirements. Annapolis. USA. 1996
- [Britt90] I. Brittain, S. N. Aksan; OECD-LOFT Large Break LOCA Experiments: Phenomenology and Computer Code Analyses, PSI-Ber.72, August, 1990.
- [Burw89] M. J. Burwell, G. Lerchl, J. Miró, V. Teschendorff, K. Wolfert; The Thermalhydraulic Code ATHLET for Analysis of PWR and BWR Systems. 4th Int. Proceedings Fourth International Topical Meeting on Nuclear Thermal Hydraulics NURETH-4. Volume 1, pp1234-1239. Karlsruhe, 10-13. October 1989. Verlag G. Braun Karlsruhe.
- [Chen77] J.C. Chen, R. K. Sundaram, F. T. Ozkaynak, A phenomenological correlation for post-CHF heat transfer. Lehigh University, Department of Mechanical Engineering. NUREG-0237. June, 1977. USA.
- [Elias98] E. Elias, V. Sanchez, W. Hering; Development and Validation of a transition boiling model for the RELAP5/MOD3 reflood simulations. Nuclear Engineering and Design. 183, pp269-286. 1998.
- [HCNo98] H. C. No, H. J. Jeong; Modifications of the reflood model in RELAP5/MOD3.1. Nuclear Technology, Vol. 124, pp52-64.1998.
- [Liles84] D. R. Liles, et. al, TRAC-PF1/MOD1, an advanced best estimate computer programme for pressurized water reactor thermal-hydraulic analysis. Los Alamos National Laboratory. NUREG/CR-2054. April 1981.
- [Lübb91] D. Lübbesmeyer; Post-test-analysis and nodalization studies of OECD LOFT Experiment LP-LB-1 with RELAP5/MOD2 cy36-02, PSI-Ber.91, NUREG/IA-00073 March 1991

-
- [NRC87] Compendium of ECC research for realistic LOCA analysis. U.S. Nuclear Regulatory Commission, Division of Reactor. Plant Systems. NUREG-1230, Volume 3. 1987.
- [R5M32] RELAP5 Development Team. RELAP5/MOD3 Users Guide. Idaho National and Environmental Laboratory. July 1996
- [Rose99] E. R. Rosal, and T.F. Lin, and L.E. Hochreiter, and F. B. Cheung, and D. E. Bessette, and J.M. Kelly; Design of the Pennsylvania State University/USNRC Rod Bundle Heat Transfer Test Facility. Transaction of the American Nuclear Society, TRANSAO 81, 1-374, November, 1999.
- [Sanch01] V. Sanchez; Validation of the Reflood Model of RELAP5/Mod3.2.2 ψ using the Data of the Integral Facility LOFT-LP-LB-1. FZK-6426. 2001
- [Sanch97] V. Sanchez, E. Elias, Ch. Homman, W. Hering, D. Struwe; Development and validation of a transition boiling model for RELAP5/MOD3 Reflood Simulation. Forschungszentrum Karlsruhe FZK. FZKA-5954. September 1997.
- [Schm85] H. Schmidt; Ergebnisse des Versuches II-B5 aus der Testserie PKL II-B5. R513/85/15. KWU. 1985

Appendix A Weisman Transition Boiling Correlation

Remarks	Equations
Heat transfer coefficient depends on distance from the quench front $h_{wl}(Z_{QF})$	$h_{wl}(Z_{QF}) = \begin{cases} h'_{wl}(TB) & : \text{ for } Z_{QF} \leq 0.1 \text{ m} \\ 0.0001 & : \text{ for } Z_{QF} \geq 0.2 \text{ m} \\ \text{interpolation} & : 0.1 \text{ m} < Z_{QF} < 0.2 \text{ m} \end{cases}$
Weisman correlation $h'_{wl}(TB)$ that depends on mass flux (G), critical heat flux (q''_{CHF}), wall temperature (T_w) and CHF-temperature (T_{wchf})	$h'_{wl}(TB) = \left\{ h_{\max} - 4500 \left(\frac{G}{G_R} \right)^{0.2} \right\} e^{-0.02 \Delta T_{wchf}} + 4500 \left(\frac{G}{G_R} \right)^{0.2} \cdot e^{-0.012 \Delta T_{wchf}}$
With following definitions:	$h_{\max} = \frac{0.5 \cdot q''_{CHF}}{\Delta T_{CHF}}, \quad \Delta T_{CHF} = T_w - T_{wchf}, \quad \Delta T_{CHF} = T_w - T_{wchf}, \quad \text{and}$ $G_R = 67.8 \frac{\text{kg}}{\text{m}^2 \text{s}}$

Appendix B FZK-Transition Boiling Model

Comments	Equations
Total transition boiling heat flux consists of contribution from heat flux to the liquid and to the vapour phase during transition boiling	$q'' = (1 - f_l \cdot M_{\text{stf}}) q''_l \cdot M_\alpha + f_l \cdot q''_l \cdot M_{\text{stf}}$
Transition boiling heat flux to the liquid q''_l	$q''_l = q''_l(p, \Delta T_s)$
q''_l represents an average heat flux during the short period of contact between the liquid and the superheated wall. A three-step process was postulated to describe the mechanisms of heat removal by a liquid film from the wall: 1) conduction heating of the liquid film, 2) nucleation and bubble growth within the liquid layer and 3) evaporation of a residual liquid film at the wall.	$q''_l = \frac{\phi_1 + \phi_{1-2} + \phi_2}{t_1 + t_{1-2} + t_2}$
Heat flux to the vapour phase	$q''_v = h_v(T_w - T_v)$
Extension of CHEN-approach to take into account low pressure (function ψ) and quality (function n) reflood situations, derived base on experimental data.	$f_1 = e^{[-\sqrt{1.8 \cdot a(\alpha)} \cdot f(G) \cdot \Delta T_s^n]} \cdot \psi(p, \Delta T_s)$ $n = 0.6 + 0.12 \cdot e^{(p/10^5)} - 0.24 \cdot x$ $\psi = 1 + 3 \cdot e^{[-0.42 \cdot p_{\text{red}}^{3/2} \cdot \Delta T_s^2]}$
Void fraction dependency of wetted area fraction (f)	$a(\alpha) = \frac{0.005}{(1 - \alpha^{40})} + 0.0075 \cdot \alpha$
Mass flux dependency of wetted area fraction (f)	$f(G) = \max(f_1, f_2)$
Mass flux dependency of wetted area fraction (f)	$f_1 = 20 - 0.6 \frac{G}{135.6}$
Mass flux dependency of wetted area fraction (f)	$f_2 = 0.2 \frac{G}{135.6}$
Limitations	$x \leq 1, \quad f_l \cdot q''_l \leq q''_{CHF}$